UPPSALA
UNIVERSITET

Digital Comprehensive Summaries of Uppsala Dissertations from the Faculty of Science and Technology 596

Digital Image Analysis of Cells

Applications in 2D, 3D and Time

AMALKA PINIDIYAARACHCHI

ACTA
UNIVERSITATIS
UPSALIENSIS
UPPSALA
2009

ISSN 1651-6214
ISBN 978-91-554-7398-3
urn:nbn:se:uu:diva-9541

Dissertation presented at Uppsala University to be publicly examined in Siegbansalen, Ångstrom Laboratory, Polackbacken, Uppsala, Friday, February 27, 2009 at 10:15 for the degree of Doctor of Philosophy. The examination will be conducted in English.

Abstract
Pinidiyaarachchi, A. 2009. Digital Image Analysis of Cells. Applications in 2D, 3D and Time. Acta Universitatis Upsaliensis. *Digital Comprehensive Summaries of Uppsala Dissertations from the Faculty of Science and Technology* 596. 57 pp. Uppsala. ISBN 978-91-554-7398-3.

Light microscopes are essential research tools in biology and medicine. Cell and tissue staining methods have improved immensely over the years and microscopes are now equipped with digital image acquisition capabilities. The image data produced require development of specialized analysis methods. This thesis presents digital image analysis methods for cell image data in 2D, 3D and time sequences.

Stem cells have the capability to differentiate into specific cell types. The mechanism behind differentiation can be studied by tracking cells over time. This thesis presents a combined segmentation and tracking algorithm for time sequence images of neural stem cells.The method handles splitting and merging of cells and the results are similar to those achieved by manual tracking.

Methods for detecting and localizing signals from fluorescence stained biomolecules are essential when studying how they function and interact. A study of Smad proteins, that serve as transcription factors by forming complexes and enter the cell nucleus, is included in the thesis. Confocal microscopy images of cell nuclei are delineated using gradient information, and Smad complexes are localized using a novel method for 3D signal detection. Thus, the localization of Smad complexes in relation to the nuclear membrane can be analyzed. A detailed comparison between the proposed and previous methods for detection of point-source signals is presented, showing that the proposed method has better resolving power and is more robust to noise.

In this thesis, it is also shown how cell confluence can be measured by classification of wavelet based texture features. Monitoring cell confluence is valuable for optimization of cell culture parameters and cell harvest. The results obtained agree with visual observations and provide an efficient approach to monitor cell confluence and detect necrosis.

Quantitative measurements on cells are important in both cytology and histology. The color provided by Pap (Papanicolaou) staining increases the available image information. The thesis explores different color spaces of Pap smear images from thyroid nodules, with the aim of finding the representation that maximizes detection of malignancies using color information in addition to quantitative morphological parameters.

The presented methods provide useful tools for cell image analysis, but they can of course also be used for other image analysis applications.

Keywords: Digital image analysis, microscopy,fluorescent staining, watershed segmentation, sub-cellular localization, point-like signals, wavelets, cell confluence, cytology, color spaces.

Amalka Pinidiyaarachchi, Centre for Image Analysis, Uppsala University, Box 337, SE-75105 Uppsala, Sweden

ISSN 1651-6214
ISBN 978-91-554-7398-3
urn:nbn:se:uu:diva-9541 (http://urn.kb.se/resolve?urn=urn:nbn:se:uu:diva-9541)

Distributor: Uppsala University Library, Box 510, SE-751 20 Uppsala
www.uu.se, acta@ub.uu.se

To my parents

ආදරණීය අම්මාට සහ තාත්තාට

Papers included in the thesis

This thesis is based on the following papers, which are referred to in the text by their Roman numerals.

I Amalka Pinidiyaarachchi and Carolina Wählby. Seeded watersheds for combined segmentation and tracking of cells. *In Proceedings of ICIAP 2005, 13th International Conference on Image Analysis and Processing, Cagliari, Italy*. Published in Lecture Notes in Computer Science (LNCS) 3617, pp. 336-343, 2005.

II Amalka Pinidiyaarachchi, Agata Zieba, Amin Allalou, Katerina Pardali and Carolina Wählby. A detailed analysis of 3D subcellular signal localization. *Cytometry A*. In press, published online, November 2008. DOI: 10.1002/cyto.a.20663.

III Amin Allalou, Amalka Pinidiyaarachchi and Carolina Wählby. Robust signal detection in 3D fluorescence microscopy. *Submitted for journal publication,* January 2009.

IV Amalka Pinidiyaarachchi, Hans Claesson and Carolina Wählby. Wavelet based estimation of cell confluence. *Submitted for journal publication*, November 2008.

V Amalka Pinidiyaarachchi and Carolina Wählby. On color spaces for cytology. *In Proceedings of SSBA 2007, Swedish Symposium on Image Analysis, Linköping, Sweden*, 2007.

Reprints were made with permission from the publishers.

The method development and writing for Paper I was performed by the author, who also presented the paper at ICIAP. In Paper II, the method development and writing was performed mainly by the author with contributions from Amin Allalou. Agata Zieba and Katerina Pardali contributed with image data and biological discussions. The idea for Paper III occurred during the work with Paper II. The method development was performed mainly by Amin Allalou in close cooperation with all co authors. The method evaluation, testing and writing were split between Amin Allalou and the author. The author contributed with the original idea, implementation of methods and method evaluation for Paper IV. Hans Claesson contributed with image data. For Paper V, the work regarding method development and writing was performed by the author.

Faculty opponent is Prof. Arvid Lundervold, Department of Biomedicine and Molecular Imaging Center, University of Bergen, Norway.

Related work by the author

I Amalka Pinidiyaarachchi, P.M.K Alahakoon and N.V.I. Ratnatunga. Feasibility of using digital image processing in the assessment of cytology smears. *In Proceedings of IITC 2006, 8th International Information Technology Conference, University of Colombo School of Computing (UCSC), Colombo, Sri Lanka, December 2006*.

II Amalka Pinidiyaarachchi, Jenny Göransson, Carlos Gonzalez-Rey, Mathias Howell, Jonas Melin, Jonas Jarvius, Mats Nilsson, Ewert Bengtsson and Carolina Wählby. Digital image processing for multiplexing of single molecule detection. *In Proceedings of Medicinteknikdagarna 2005, (A biomedical engineering meeting) Stockholm/Södertälje, Sweden, September 2005*.

Contents

1. Introduction

The rapid growth in digital imaging techniques associated with light microscopy allows researchers from the fields of biology, medicine etc. to produce large amounts of image data in a variety of experiments. This sometimes overwhelming amount of image data needs to be handled carefully to allow the extraction of the required information in a resourceful manner. Thus the role of image analysis is not limited only to the analysis of the acquired image. In many instances, it also extends to working together with those who acquire images, to make decisions on the best approach to produce the image data at the microscopes. It is always better for the image analysis to start with "good quality images" rather than trying to "make them good" for processing later. It is also important to decide when to perform an analysis in 2D and when it is necessary to extend it to 3D. Images in 3D not only mean more data and more storage requirements but they also demand extended methods for analysis and more memory and processing power to handle the large amount of data when performing the analysis.

Over the past years experts from the fields of biology and medicine, and image analysis have worked together to produce various important research results in close collaborative manner that has benefitted both sides. The work that led to this thesis can be seen as an addition to the same endeavor and is hence entitled "Digital Image Analysis of Cells - Applications in 2D, 3D and Time". The main aim is to investigate and extend existing image analysis methods for new applications and also to 3D where necessary. New methods that outperform existing methods have also been investigated. The image data used in this thesis shows cells from different experiments and the images were obtained using different microscopy techniques both in 2D and 3D. In a time series of images the time accounts for an additional dimension.

When tracking of live cells in time-lapse images is needed in order to investigate the growth of the cells, time can be thought of as the third dimension of a 3D data set. The tracking process then involves dealing with cells that divide, merge and group into clusters over time. Paper I describes a method for performing a combined segmentation and tracking on live cell images. With the advent of new techniques in fluorescence microscopy, biologists are able to tag specific protein complexes inside cells with high specificity. Studying such complexes inside cells requires images acquired

as 3D stacks and image analysis methods to localize the signals also in 3D. This type of 3D nuclei segmentation and point-like signal localization method is presented in Paper II. Paper III is a continuation of the work on the point-like signal detection method where the performance of the method is evaluated. Live cell imaging does not limit the requirements of image analysis to segmentation and tracking only. Sometimes the main aim is to obtain quantitative measurements on the samples over time. Cell confluence, i.e., the percentage of live cells that covers the cell growing surface, is an important measurement for certain experiments. Texture analysis based confluence measurements are discussed in Paper IV. Staining biological samples with dyes with the aim of increasing contrast at the bright-field microscope is a common practice in some experiments. This additional color information associated with the images can sometime be used in the image analysis tasks as well. Paper V is an attempt to explore this aspect of use of color for cytology.

This thesis is organized as follows: Section 2 is an overview of different microscopy techniques and the different methods used in staining. Section 3 includes the discussion on the image analysis concepts that are in focus in this thesis. The contributions by the author are included in Section 4 with the concluding remarks and future work following in Section 5. A brief summary of the papers included in the thesis can be found in Section 6.

2. Microscopy of cells

Cells and the internal structures of the cells can be observed using many different forms of light microscopy ranging from the normal bright field microscopy to advanced systems like the Stimulated Emission Depletion microscopy (STED) (Davidson and Abramowitz, 2008, Klar *et al.*, 2001). With the advances of the Green Fluorescent Proteins (GFP) (Tsein, 1998, Cantrill, 2008) a whole new color palette becomes available for fluorescence microscopy enabling the study of protein dynamics and functioning in living cells. The applicability of this wide range of techniques in a particular situation differs depending on the questions asked and also the availability of the techniques. The cell images used in the work presented in this thesis were acquired using bright field and confocal fluorescence microscopy in their common forms of use. The actual settings of the microscopes (e.g. having special contrast methods for bright field microscopy) and the type of staining used (to increase contrast in the bright field or to specifically tag components in the cells in fluorescence microscopy) have been decided by the experts involved. This chapter covers a brief description on the microscopy methods involved and the details related to their settings in the relevant experiments.

2.1 Bright field microscopy

The human eye is capable of seeing differences in signal amplitude, perceived as brightness and difference in wavelength perceived as color. A bright field microscope uses these two types of differences in creating an image of the sample. Only the specimens that have some property that affects the amount of light that passes through, can be visualized using these types of microscopes. A simplified diagram showing the light path of a normal bright field microscope is shown in Figure 2.1 (A). A set of lenses, i.e., collector lens (a) and condenser (b) collects and directs light from light source on to the specimen and then the light passes through objective (c), tube lens (d) and projection lens (e) and gets collected on the detector. The magnification, i.e., how large the final projection will be, is decided by the magnification provided by the objective.

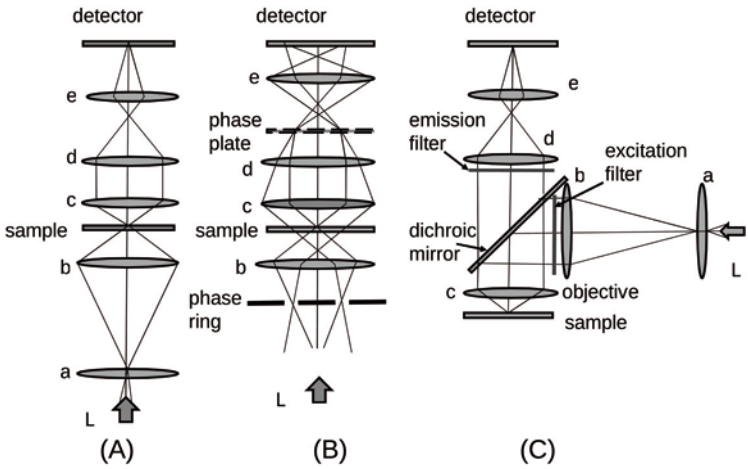

Figure 2.1: Simplified diagrams for different microscopes. (A) Normal bright field, (B) Phase contrast, (C) Fluorescence. L is the light source.

To increase the contrast specimens can be stained with color and this often requires fixation of the specimen meaning that the cell are dead. There are a number of stains that can be used and all the colors used for staining different structures will be registered in the same image. In the study of color spaces for cytology in Paper V, the cytology smears have been stained using Papanicolaou staining (nuclear stain haematoxylin (blue) and cytoplasm staining eosin (pink/red)) to clearly visualize the cell nuclei. The main concern in the study is to find malignant samples, and color, in addition to the other quantitative parameters, can provide information on the malignancy. See Figure 2.2 (A) for an example of what this type of staining looks like.

In live cell imaging that uses normal bright field microscopy, the increase of the contrast level can also be acquired in other ways. This use of additional methods to increase the contrast is desirable especially in cases where the samples are faint and the absorption is not evident. The contrast in such cases is caused by refraction rather than absorption. The stem cell images in Paper I imaged under bright field microscopy, have been imaged with a slight defocus to achieve higher contrast at the cost of lower resolution, see Figure 2.2(B). The theory behind this approach is explained in detail in Degerman (2005).

If live cells need to be imaged as a time sequence and imaging is performed on several parts of the specimen, the best approach is to use an automated microscopy system. This will minimize the errors that can be made by manually changing between the different locations of the specimen. A system performing live cell imaging, needs a specially controlled environment that mimics the cells' natural environment for the cells to stay healthy. A practical

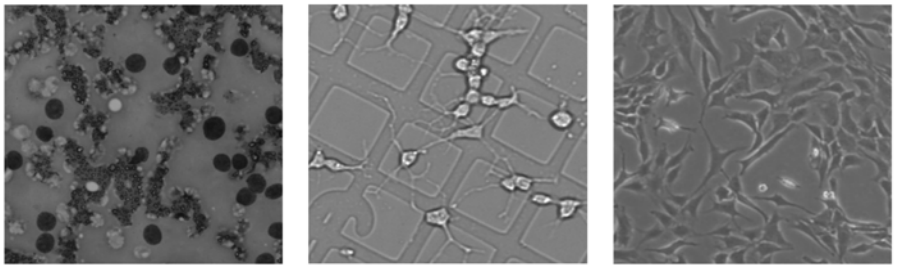

Figure 2.2: Images obtained using different contrast enhancement methods at bright field microscopy. (A) using staining to increase contrast (Paper V) (see Figure 4.10(A) for color image), (B) using slight defocus (Paper I), (C) using phase contrast microscopy (Paper IV).

system also has to have the ability to perform the auto-focusing in a suitable manner. If such an auto-focus mechanism is not used, another option is to acquire a stack of images from different focal planes for each section. This stack can then be used later, to obtain the best slice by an auto-focus function (Brenner *et al.*, 1976) searching for the optimal focus position based on local image contrast. This approach has been used in obtaining the images with best contrast from the time-lapse image sequence of stem cells used in Paper I. See Althoff (2005) and Degerman (2005) for further details.

2.2 Phase contrast microscopy

There are special techniques that have been developed in order to increase the contrast with bright field imaging, namely phase contrast and differential interference contrast (DIC) (Davidson and Abramowitz, 2008). These techniques use optics in order to increase the contrast and therefore can be used for live cell imaging also as time sequences.

When light passes through the specimen, the beams that come into contact with objects change the phase relative to those that pass through empty spaces. The difference introduced by the specimen is only approximately one-quarter wavelength and the destructive interference caused these diffracted and undiffracted light is not enough to make an image visible. Phase contrast microscopy uses a phase ring and a phase plate to selectively introduce an additional one-quarter wavelength to the undiffracted beam before it recombines with the diffracted beam. The destructive interference of these two beams can now be seen as difference in brightness on the image. Figure 2.1(B) shows a simplified diagram of the setup of a phase contrast microscope. This type of microscopes are widely used for live cell

imaging and time-lapse imaging. They have the advantage over other light microscopes of being able to produce high contrast image data without disturbing the cells by staining and/or fixation. The images of fibroblasts used in the confluence measurements of Paper IV are positive phase contrast images obtained using an inverted microscope, see Figure 2.2(C).

2.3 Fluorescence microscopy

Fluorescence microscopy has become an indispensable technique for performing precisely localized detection of interactions within the cells. The microscopy and imaging need to be associated with specially designed techniques and the advances in both have enabled the study of dynamic processes in living cells (Stephens and Allen, 2003). The schematic diagram for a fluorescence microscope is shown in Figure 2.1(C). The fluorescent molecules in the stained sample absorb light of a certain wavelength and emit light of a longer wavelength. The dichroic mirror reflects light below a given wavelength while transmitting the light of longer wavelengths. Together with the excitation and emission filters, it is possible to expose the sample to only the light of the absorption wavelength and to only let the emitted light of the specific wavelength to be captured at the detector. This enables capturing parts stained with different flourochromes as images in different channels.

In wide-field fluorescence microscopy the whole sample is illuminated and the incoming light from out-of-focus parts also gets collected on the image. This is problematic especially in 3D since the quality of the images become poor making the image analysis tasks more complicated, see Figure 2.3(A) for a DAPI (4',6-diamidino-2-phenylindole) stained cell nucleus form preliminary tests of Paper II, imaged using wide-field microscopy.

2.4 Confocal microscopy

The technique of confocal microscopy is similar to normal fluorescence microscopy but with the addition of pinholes both at the light source and the detector that removes out-of-focus light. This will increase the z resolution.

The image data for Paper II were acquired using confocal microscopy. During the first sample experiments the image acquisition was performed using wide-field microscopy with DAPI as the nuclear satin, see Figure 2.3(A). As can be seen the extraction of the exact boundary in z direction is impossible. New model based segmentations were tried, e.g., using an ellipsoidal model that needs the initial input of the approximate center slice form the user. This gives visually appealing results but the

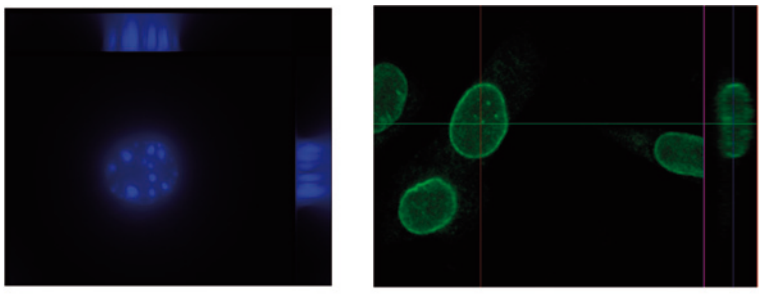

Figure 2.3: (A) A DAPI stained nucleus imaged at wide-field microscope, xy slice, xz and yz projections showing the effect of out-of-focus light. (B) nuclei imaged under confocal microscopy, visualized using anti-Lamin B1 and FITC, and one nucleus with the yz projection showing the improved z resolution.

output depends on the user inputs and the importance of extracting the exact boundary led us to switch to confocal fluorescence microscopy to acquire the image data. Figure 2.3(B) shows a cell nucleus from image data of Paper II visualized using anti-Lamin B1 and FITC, imaged at a confocal system. The figure shows an xy slice and the corresponding yz projection. The main disadvantages of confocal microscopy are the significantly lower light collection efficiency and the longer image acquisition time.

2.5 Point Spread Function

The resolution, i.e., how close two objects can be within an image and still be resolved as two distinct objects, depends on the imaging system properties, particularly on the point spread function (PSF). For a given microscopy system the PSF is usually modeled with a Gaussian function (Zhang *et al.*, 2007) and the full width at half maximum (FWHM) of the PSF is used to measure resolution. The determined PSF can be used to reassign the out-of-focus light mathematically (Bolte and Cordelieres, 2006). This is known as deconvolution and is available as an option at some microscope systems.

When the PSFs of wide-field microscopy and confocal microscopy are compared, confocal systems show improved resolution in both axial and lateral directions. The z resolution is still poor compared to the xy resolution. This has to be taken into account when performing image analysis. For example, the 3D filters used in Paper III that detect and verify point-like signals, were altered in the z direction to compensate for this anisotropy.

2.6 Staining techniques

When biomolecules are analyzed quantitatively, a priori knowledge about the analyte is used, and the target is recognized by using a specific affinity reagent. For proteins, these affinity reagents are usually anti-bodies and the target can be detected using a fluorescence labeled antibody, see Figure 2.4(A). The specificity, i.e., the degree to which a correct analyte is measurable, depends on the specificity of the antibody and the specificity of the detection method. To increase the signal-to-noise ratio (SNR), target detection can be associated with a secondary antibody, see Figure 2.4(B). Thus the process, in simple would be to capture a protein by an antibody and to target the antibody by a secondary fluorescently labeled antibody (Alberts *et al.*, 2002). As opposed to these artificially introduced fluorescent molecules, the Green Fluorescent Protein (GFP) which is fluorescent itself, can be used for tagging proteins in living cells.

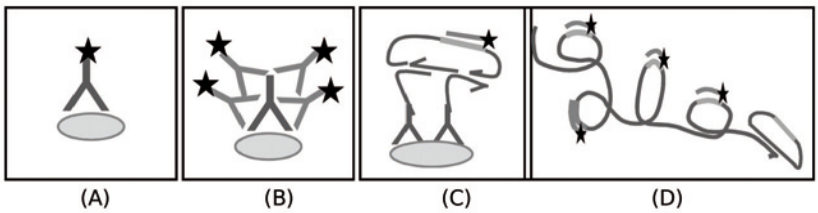

Figure 2.4: Staining techniques for protein detection using (A) a fluorescence labeled antibody. (B) secondary antibody to achieve high signal to noise ratio. (C) and (D) using Proximity Ligation Assay.

2.7 Proximity Ligation Assay

The in situ Proximity Ligation Assay (PLA) is a protein detection method based on target recognition by two or more antibodies. PLA converts the recognition of a protein complex by two or more antibodies into a circular DNA molecule (Söderberg *et al.*, 2006). This circular DNA molecule is then amplified using so called rolling circle amplification, and the localized concatameric product is detected using fluorescent DNA probes. Protein complexes that are detected by in situ PLA have the combined effect of highly specific target recognition with a high SNR. The point-like signals analyzed in Paper II (Smad complexes) and Paper III (AuroraB-Survivin complexes) originate from protein complexes are detected using PLA, see Figure 2.4(D) and (E).

3. Fundamental image analysis concepts

Digital image processing can be thought of as a sequence of steps: image acquisition, pre-processing, segmentation, feature extraction, analysis and evaluation. These steps can also be expanded into more intermediate steps depending on the application. For example, the sample preparation can also be thought of as an initial step prior to image acquisition. There can also be steps that can be categorized as post-processing. The author was not directly involved in image acquisition except for some initial tests performed for optimal settings for images used in Paper II. The microscopy techniques used for image acquisition are discussed in Section 2. The focus in this section is on the steps after image acquisition and the related concepts.

3.1 Digital image data

A digital image is generally represented with a square grid consisting of picture elements (pixels) in 2D and in 3D the elements are referred to as voxels. Each element has a value that describes the content of the position of the imaged object that it represents. In a binary image the value is either 1 (part of an object) or zero (part of the non-object or background regions). In a gray valued or gray scale image the range of values change depending on how the structure that stores the information is defined. If an 8-bit representation is used 2^8 is the upper limit and each element can have a value ranging between 0 and 255. This is the most common form of representation but it is not so uncommon to use other representations such as the 16-bit representation that gives a value between 0 and 65535. The appropriate representation can be decided based on the amount of information needed to represent the object of interest and also the amount of storage available.

A color image follows the same structure with the addition that, instead of having a single number representing a gray value, each element has a value for each color component. In an RGB (Red, Green, Blue) representation three values represent how much red, green and blue are contained in each element. In essence this means that instead of one matrix of values (in 2D) we have three matrices of gray values, one for each color component. However, the number of colors, or spectral channels does not need to be

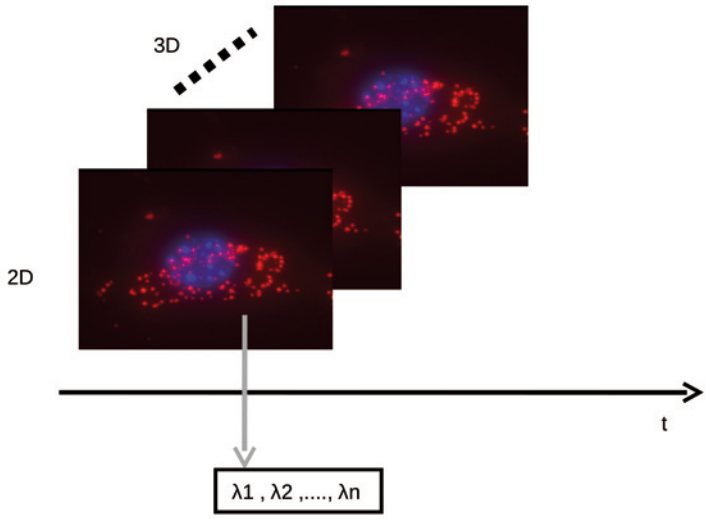

Figure 3.1: Digital images and the different dimensions; 2D, 3D, temporal (time, t) and spectral (color, λ) dimension.

limited to three and there are various application such as remote sensing, that use multispectral imaging. It is sometimes used in fluorescence microscopy as well.

A set of images collected over time will have an additional dimension, the time. An important issue in acquiring these time-lapse sequences is the temporal resolution that defines the rate at which the images are acquired. A suitable rate should be based on the viability of the live cells imaged. (Meijering *et al.*, 2008).

Putting things together more formally, a digital image can be represented as a discrete integer-valued function $f(x); x = (x, y, z, t, \lambda)$ where *x, y, z* are the spatial coordinates, t the time component and λ the color component. Figure 3.1 shows representations of digital images in different dimensions.

3.2 Spatial domain and frequency domain

The image or image volume representations described above are also referred to as spatial domain representations. One alternative is the frequency domain where the image content is represented as frequencies. In general, slowly varying intensity components in the spatial representation are represented as low frequency components while sharp transition in intensity are represented as high frequency components. The Fourier transform maps the spatial domain representation of an image into the frequency domain representation.

The general form of the Fourier transform is shown in Equation 3.1. In the discrete case the Fourier transform can be obtained by correlating the input signal *f(t)* with the sinusoidal basis functions whose frequencies are determined by the values of ω, see Equation 3.2.

$$F(\omega) = \int_{-\infty}^{\infty} f(t) e^{-i\omega t}\, dt \tag{3.1}$$

$$F(\omega) = \sum_{t=0}^{N-1} f(t)[cos(2\pi\omega t/N) - sin(2\pi\omega t/N)] \tag{3.2}$$

where N is the number of samples. The duality between the spatial domain and frequency domain allows performing a given operation such as filtering on either of the domains to obtain similar results. However, in certain image analysis tasks it is convenient to use the frequency domain representation of the image rather than the spatial representation. For example, the point-like signal detection discussed in Paper II and III make use of this representation in the first harmonic of the Fourier series and convolve an image with cosine and sine filters to detect and verify point-like signals.

3.3 Pre-processing

Pre-processing, as the name suggests, alters the content of the image and makes it more suitable for the following image analysis steps. The aim of this step should however not be to make the images "look nice" since by doing so, one might risk throwing away useful information, but rather to make them more suitable for the next steps to be applied. One common example of a pre-processing step is noise reduction. Filtering in spatial domain, performed in a controlled manner will decrease the effect of noise on images. A meaningfully designed smoothing filter will even out the noise in an image without blurring important information such as edges. Median filtering, that determines filter output coefficients by the median of the neighboring pixels/voxels, is a non-linear filtering method that preserves edges. However median filtering suppresses fine details. Three commonly used edge preserving smoothing filters are SUSAN (Smith and Brady, 1997) and bilateral filtering (Thomasi and Manduchi, 1998) that combine range (intensity difference) and domain (spatial distance) filtering, and anisoropic diffusion that uses a modified scale-space approach (Perona and Malik, 1990). We use anisotropic diffusion as a pre-processing step prior to cell nuclei segmentation in the 3D signal localization of Paper II. Figure 3.2 shows the difference between Gaussian smoothing and anisotropic diffusion applied to an image. The Gaussian

mask is circularly symmetric and the filtering thus, is isotropic. Note how the edge information is preserved by anisotropic smoothing.

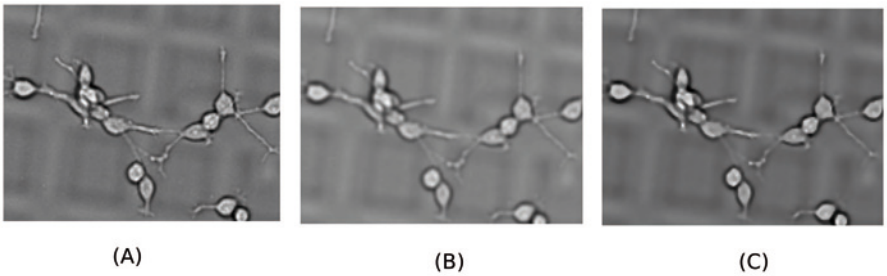

Figure 3.2: (A) Original image. Smoothing using (B) a Gaussian mask (C) anisotropic diffusion. Note the edges that remain sharp in (C).

3.4 Image segmentation by gray value thresholding

Image segmentation is the process that separates the content in an image into objects and background, and can be seen as an essential part of many image analysis tasks. Depending on the type of images, the segmentation can be either simple and straightforward or extremely difficult or somewhere in between. It is image analyst's task to select the method that gives the best result for the given task.

Thresholding is a popular image segmentation method. There are a number of automated thresholding techniques that perform global thresholding, i.e., thresholding an entire image with a single threshold. In local thresholding, the image is partitioned into sub regions and thresholding is performed on each part separately. A comparison of different thresholding methods can be found in (Sahoo *et al.*, 1988). In the case of having bright objects in a dark background, the pixels/voxels of the image that have values greater than or equal to the selected threshold (gray value) will be set as objects while the rest of the pixels/voxels are set as background. More formally, a given image $f(x)$ will be converted to the binary image $g(x)$ by selecting a gray value T such that

$$g(x) = \begin{cases} 1 & \text{if } f(x) \geq \mathrm{T} \\ 0 & otherwise \end{cases} \tag{3.3}$$

where $min_x f(x) \leq \mathrm{T} \leq max_x f(x)$

This process is also known as binarisation. An efficient way to find the best threshold T for an image is to look at the distribution of the gray values in

the image histogram. A popular thresholding method based on the histogram is Otsu's (Otsu, 1979) where the automatic selection of an optimal threshold is performed based on the class seperability of the histogram. If an image contains objects with fairly similar gray values that are significantly different from those of the background, the histogram will have two distinct peaks with a valley in between. A gray value close to the valley can then successfully be used to separate the objects from the background. However, if the objects and background have overlapping intensities then the histogram will not have distinct peaks and finding the optimal value for thresholding is difficult. Image pre-processing can be useful in reducing the variations in the gray values within objects and also within the background to increase the between class separability.

However, if an image contains objects that are close together, the thresholding will fail in segmenting each object separately. This leads to defining image segmentation as a twofold issue, i.e., segmenting objects from background and segmenting individual objects. In most of the situations, image segmentation means accomplishing both these, segmenting objects from background as well and segmenting individual objects if they are close to each other.

Thresholding does not necessarily need to be performed on the original gray scale image. Other measures can be used to transform the image into a different domain that introduces higher inter-class variability to the data. One such example is the use of local variance of the gray levels on the image. This method simply computes a variance image from the original based on local variance of gray values within a defined mask. The areas with high variance will get higher values while those with rather uniform values get lower values. This can be a good choice to separate objects from background in the cases where image objects contain a lot of internal structure and are surrounded by a more uniform background, see Figure 3.3. However, separation of closely lying object might still be an issue for this approach.

3.5 Watershed segmentation

When a simple thresholding method is insufficient for accurate image segmentation, extended methods have to be explored. We describe one such widely used method, the watershed segmentation, which has been used in some of the work presented in this thesis (Papers I, II and V).

Watershed segmentation was originally presented as a contour detection method by Beucher and Lentuéjoul (1979) and has later been refined to work more efficiently by Vincent and Soille (1991). The concept has been adapted to work equally well both in 2D and 3D segmentation tasks. Watersheds can be applied on various types of images such as directly on the gray value image, on a distance transformed image, or a gradient image, in order to

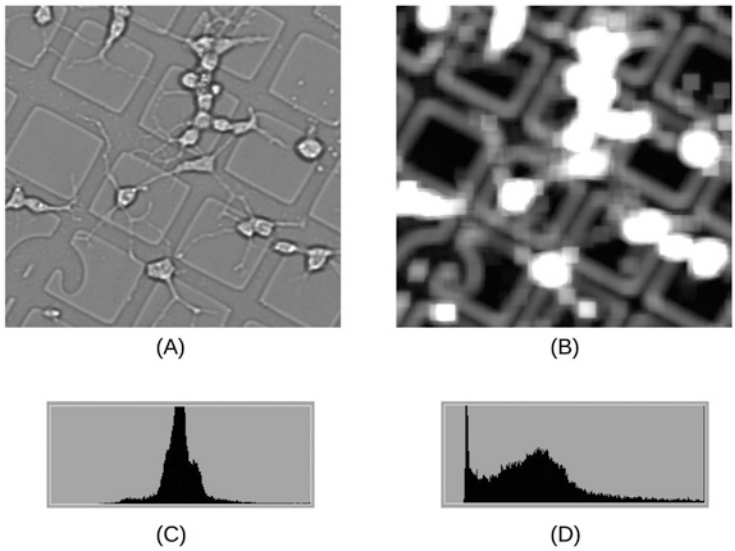

Figure 3.3: Original image with overlapping object and background intensities. (B) The variance map, obtained using a square mask, that increases the inter-class variability.(C) and (D) The corresponding histograms.

divide the image into a set of meaningful regions. The general idea is to consider the image as a landscape where the magnitudes of the gray values form the hills and valleys of the landscape. The watershed segmentation starts by submerging the landscape in water, and water is allowed to rise from each minimum. When two water fronts from different minima meet, a dam is built in between. These dams, or the watersheds, are the segmenting lines for the different regions. In the case of applying the method on gray scale images that are comprised of bright objects in a dark background, the method is applied on the inverted image. If there are touching objects with a faint border in between, the water from one catchment basin can leak into the other, merging the two objects and labeling them as one. This is commonly known as "under segmentation". In addition, if the objects have internal structures there will be more than one minimum for a given object. This means one object will have water rising from more than one minimum dividing it into several parts. This second common defect is termed "over-segmentation". Several approaches have been used in minimizing these two types of errors. One common approach to minimize the amount of under segmentation is, allowing a certain amount of over segmentation that is treated later in a refinement step.

The general concept of rising water is actually a region growing criteria in the image processing terminology. What is different from the normal region growing is that instead of working on neighborhood layers, watersheds work on intensity layers. Since the concept of watersheds was first introduced to

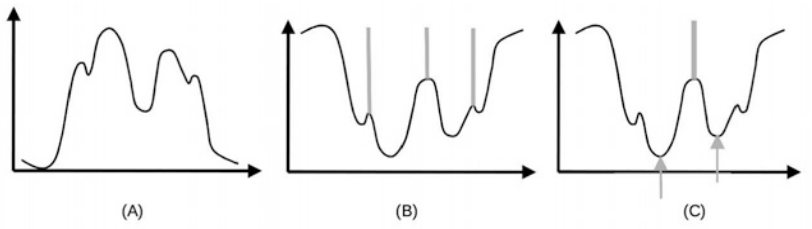

Figure 3.4: A simple 1D illustration of seeded watersheds. (A) 1D intensity profile, (B) Inverted intensity profile with resulting watershed lines (dams), shown as gray lines, obtained by allowing water to rise from each local minima, (C) Reduced oversegmentation achieved by selective seeding, indicated by arrows.

image processing, there have been a vast number of modifications and refinements that have been incorporated with it to obtain a successful segmentation. The improvements by Vincent and Soille (1991) are concerned with making the method fast and efficient by using sorted pixel arrays in the region growing. Marker controlled, or seeded watersheds (Vincent, 1993) is probably one of the most successful refinements incorporated to the method. It enables selective region growing based on an initial seeding, allowing water to rise only from the pre-defined seeds instead of from every minima, yielding much less over-segmentation. See Figure 3.4 for a simplified 1D illustration of this. The seeds can be defined either manually or using an automated method (Lindblad *et al.*, 2004, Wählby and Bengtsson, 2003, Wählby *et al.*, 2004). With seeding under-segmentation can be eliminated almost entirely, provided a careful selection of seeds. The over segmentation and false segmentations caused by extra structures in the image still need to be treated. Figure 3.5 shows seeded watershed segmentation. Objects seeds are found using the h-maxima transform (Soille 1999) that suppresses all intensity maxima whose height is less than a given threshold value h. Background seeds are found thresholding the variance image in Figure 3.3(B). These seeds are used in the watershed segmentation that gives the result in (B).

The detected false objects and the over segmentation can be treated in various ways. If the information on approximate object size is available, a size threshold can be used to remove some of the false objects. Some over segmented regions can be merged with either the background or the objects using merging criteria that preserve the strongest edges, i.e., merging regions with weak borders. See Figure 3.5(C) for the final result after merging objects with weaker borders.

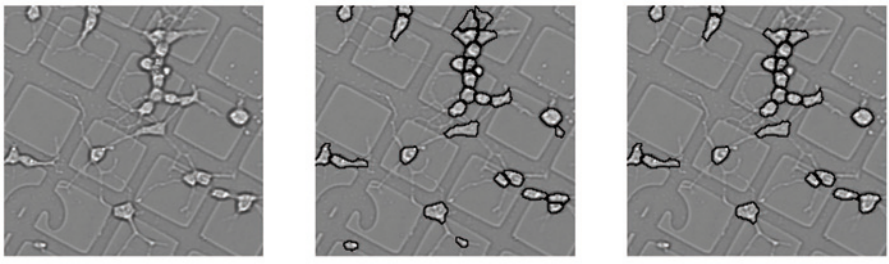

Figure 3.5: Seeded watershed results. (A) Original image, (B) Result after applying seeded watershed segmentation. Objects seeds found by the h-maxima transform and background seed from thresholding the variance map shown in Figure 3.3 (B). (C) Final result after applying the merging step.

3.6 Texture analysis

Another field of image analysis is the texture analysis (Sonka, 2007, Tuceryan and Jain, 1993). The primary concern in texture analysis is extracting a set of features from the texture in order to perform a classification on the image data. The aim of the classification is to derive conclusions about the image data. The set of features extracted from a given texture should sufficiently describe the texture and distinguish it from the rest of the textures present. In addition to the use for classification, texture analysis can also be used as an image segmentation method. In fact, one can think of gray level based segmentation as segmentation based on classification.

3.6.1 Feature descriptors

The most important and often difficult task in texture analysis is to determine the best set of feature descriptors to describe and discriminate between the textures of a given image. The simplest are the first order statistics such as mean and standard deviation, that can be computed from the gray level histogram of the image. An early study of textural features for image classification was carried out by Haralick *et al.*, (1973) where they propose the use of a gray-tone spatial-dependence matrix, also more commonly known as the graylevel co-occurrence matrix (GLCM). The idea is to assume that the texture based information in an image is contained in the overall, or average spatial relationship, that the gray levels in the image have to one another. After calculating the co-occurrence matrix, a set of features are derived from the matrix in order to classify the image. The set of features described in (Haralick *et al.*, 1973) are often referred to as "Haralick" features and are used extensively in various texture analysis tasks

(Szczypiński *et al.*, 2008). Local binary pattern (Ojala and Pietikäinen, 1995) is another popular second order statistic used in various texture classification tasks. In the context of cell image analysis, classification methods based on texture have been used in various tasks such as quantifications on histological studies and cervical cancer diagnosis (Abella *et al.*, 2008, Schilling *et al.*, 2007) and also in nuclei classification in 3D (Kim *et al.*, 2007).

3.6.2 Wavelets for texture analysis

In addition to spatial texture analysis, frequency based methods have also been used in some applications (Arivazhagen and Ganesan, 2003, Chang and Kuo, 1993). The basic idea behind wavelets is to analyze depending on the scale, i.e., analysis is performed on different scales or resolutions. This enables the performance of multiresolution analysis on the image data that would reveal textures that otherwise wouldn't be prominent. The Fourier transform which is also frequency based has sinusoids as basis functions as seen in Section 3.2. This makes the Fourier transform reveal only the frequency information as opposed to wavelet transform that uses of locally oscillating basis functions called "wavelets" that could reveal both frequency and spatial information.

The wavelet transform convolves a given signal with a set of shifted and scaled versions of the initial wavelet. At each scale the approximation coefficients are generated by a low pass filter and the detailed coefficients, from a high pass filter. In other words, the the low-pass filtered signal is a coarse representation while the high-pass filtered signal contains details. The discrete wavelet transform (DWT), applied on images are 2D transforms that analyze image across the rows and columns that separate horizontal (low pass filtering of the rows followed by high pass filtering of columns), vertical (high pass filtering of the rows followed by low pass filtering of columns) and diagonal details (high pass filtering on both). This is represented as a schematic diagram in Figure 3.6 and Figure 3.7 shows the result of applying DWT on an image.

In the general texture analysis methods based on wavelets, the image is decomposed into subbands in the first level and either the low frequency channel decomposition or selective decomposition of a certain frequency channel can be performed in the next levels. The feature sets calculated from the subbands can once again be the co-occurrence features or first order statistics like mean and variance or a combination of both (Arivazhagen and Ganesan, 2003).

Complex wavelets have better shift-invariance and better directionality compared to the real wavelets. The implementation by Kingsbury (1998, 2001), the DT-CWT, uses two trees of real wavelets to make the real and

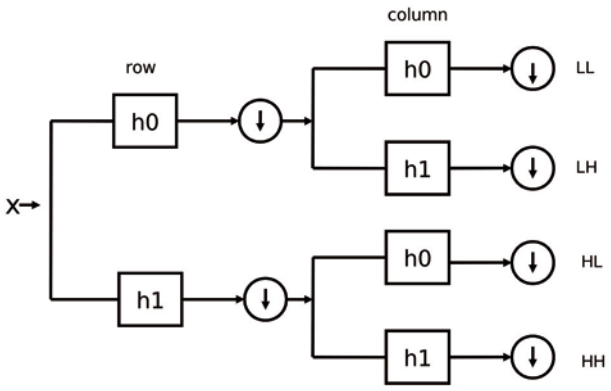

Figure 3.6: Wavelet decomposition tree in 2D showing one level. Input X, the filters low-pass (h_0) and high-pass(h_1) and the four subbands LL,LH,HL and HH. The down arrow indicates down-sampling.

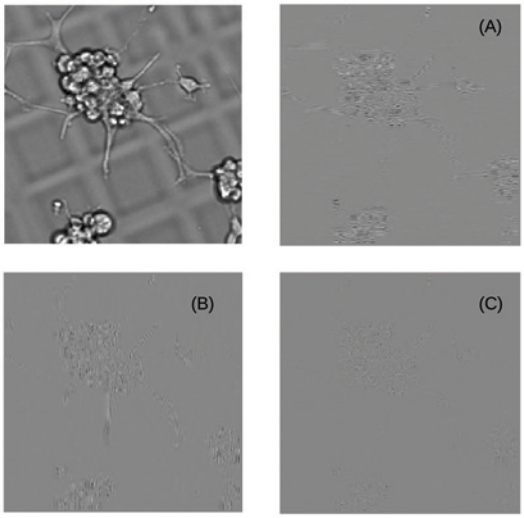

Figure 3.7: Discrete wavelet transform (A) Original image (B) Horizontal details (C) Vertical details and (D) Diagonal details.

imaginary parts of the coefficients separately. This can distinguish directions in different orientations compared to the real wavelet. This form of wavelet transform has been used not only in image processing applications such as image compression and noise reduction, but also for texture analysis (Hatipoglu *et al.*, 1999). The issues related to designing the filters is described in detail in (Selesnick, 2005). A version of the DT-CWT approach, namely the real oriented dual tree wavelet transform (real oriented DT-CWT) described by Selecsnick *et al.*(2005) is used to obtain the six directional subband in Figure 3.8. As the name suggests, two parallel trees using two

different sets of specially designed filters give six detail sub-bands. The sum and difference of these sub-bands give the six directional oriented outputs.

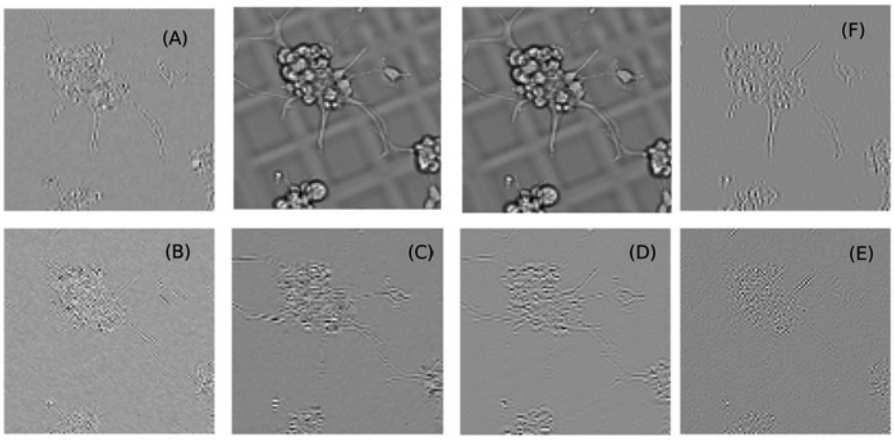

Figure 3.8: The DT-CWT subbands in first level . In the middle, the two approximations from the two trees. (A)-(F) The six oriented subbands in -75°, -45°,-15°, 15°, 45° and 75° respectively.

3.7 Color image processing

Color, as humans perceive it, is the response from the three different spectral sensitivity ranges of the cones in the eye. Therefore most imaging devices are designed to optimize this tristimuli , red , green and blue (RGB). However, in image analysis we can have not only three but multispectral, i.e., number of spectral channels depending on what we want to analyze in the acquired images (Åhlen, 2005). Most gray level image segmentation techniques can be extended to color images as well. The methods such as histogram thresholding, edge detection, fuzzy approaches etc. can be applied to each component of the color image separately and combined to obtain a final result. However, when a color image is separated to the three color components R, G and B, the color information is scattered and the information that humans can perceive is lost. When compared to gray scale images, color images have additional information that can sometimes be useful or even necessary in image analysis tasks (Ranefall, 1998). There are other color spaces representations such as HSV (hue, saturation, and value/intensity) that are commonly used. In HSV, color is represented by hue and saturation and is separated from intensity which makes it more useful, e.g., in image enhancement since the algorithm can be applied to intensity component only, without affecting the color information. The CIE color system is a scheme that represents perceptual uniformity of

color. It consists of three primaries X, Y and Z and a combination of these three can be used to specify any given color. CIE_{Luv} and CIE_{Lab} are two color spaces obtained using non-liner transformations of X, Y and Z values. Each of these color spaces have certain advantages and it is often a non-trivial task to decide which color space gives the best result in analysing the features in an image. (Cheng *et al.*, 2001).

4. Applications methods and results

In this section the methods and results of the included papers are presented briefly. The fundamental concepts are discussed in the previous section and this section discusses the application of the methods and the obtained results.

4.1 Seeded watersheds for cell segmentation and tracking

Paper I and Paper II

In cell migration analysis cells need to be tracked along a time-lapse sequence of images. Performing this type of tracking manually is time consuming, tedious and error prone. Therefore an automated cell tracking scheme is preferred. The image analysis task in such cases is generally twofold; segmentation and tracking. In previous studies watersheds have been used in this type of analysis, but as a segmentation tool applied on each image separately. Matching algorithms are thereafter used, to track the cells through time.(De Hawver *et al.*, 1999) Our approach in Paper I is to use the seeded watersheds for both segmentation and tracking of cells where the segmentation result from the previous time frame is used to create seeds for the current frame.

The image data used in this work is from a study investigating the mechanism behind the differentiation of the neural stem cells and consists of 30 different sequences. The correctness of the initial segmentation is important for the subsequent steps since the tracking is performed by propagation of the seeds. The aim of this analysis is to track the cells through splitting and merging of cells. The method is capable of dealing with splitting and merging by correctly labeling and tracking of the cells with a rule based criteria.

The seeded watershed algorithm requires initially defined seeds to start the segmentation and in our implementation we use both object and background seeds. As can be seen from the original image in Figure 4.1(A), thresholding will fail to optimally distinguish objects and background. As discussed in Section 3.4, a variance thresholding method applied on the images will allow successful definition of the background seed. Object seeds at the initial step are found using the extended h-maxima transform [Soille, 1999] that filters out local maxima using a contrast criterion. An h value that gives satisfactory results is selected by visual inspection on some test data and is kept fixed

for all image data. Figure 4.1(B) and (C) shows the variance image and the selected object and background seeds for the original image in (A). The initial result from watershed segmentation and the refinements applied to it as discussed in Section 3.5 are shown in Figure 4.1(D), (E) and (F). The result shows the advantage of having seeds. Seeding is used to initiate the segmentation. It is also used as a criterion to remove over-segmentations that occur due to non seeded intensity maxima, see Figure 4.1(E). This is achieved by region merging, applied as a second step after initial segmentation.A region is merged with the neighboring regions towards which it has a weaker border. This merging is carried out until all non seeded objects are merged, either with the background or objects.

On the other hand if less number of seeds is defined this step might result in under segmentation removing some of the correctly segmented objects. If an automated method is used to define the initial seeds it is therefore always preferred to have extensive seeding. As can be seen in Figure 4.1(C), we use extensive seeding that gives more than one seed for some cells. The over segmentation caused by this extensive seeding is removed by a third step where region boundaries crossing bright parts of the image, e.g., a boundary dividing a bright cell in two, are removed, see Figure 4.1(F). In this case we continue the merging until all remaining objects have a maximum average intensity along the border. This step will not only reduce over-segmentation, but also merge false objects, such as debris, with the background.

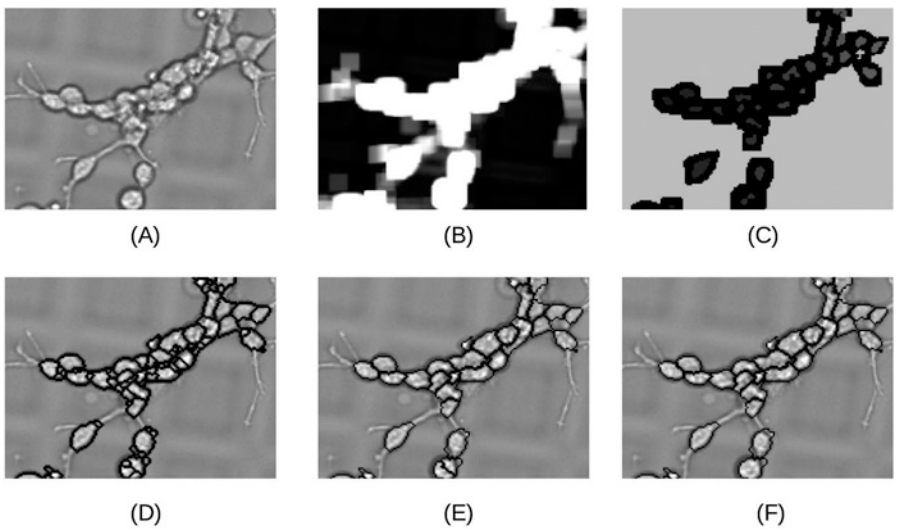

Figure 4.1: Cut-offs of the images showing the steps of the watershed segmentation. (A) Original image, (B) Variance map, (C) Object seeds (dark gray) and background seeds (light gray), (D) Initial watershed result with over segmentation, (E) After removing non seeded objects, (F) After merging over-segmented objects.

The result from watershed segmentation and merging, have labeled regions corresponding to each of the cells in that frame. These regions are used to define what we call the "centroid seeds" by obtaining the centoid of each region. These centroid seeds are then dilated using a 3x3 structuring element. For the next frame, the "h-maxima" seeds are obtained as previously described. For cells to be tracked, these h-maxima seeds need to carry the corresponding label from the previous frame before using them in watershed segmentation. Thus, each centroid seed is compared with h-maxima seeds of the next frame. This is performed in a sequence of steps as follows. First, the indexes of centroid seeds are obtained. Then for each indexed pixel in each region, the neighborhood indexes of the eight neighbors are taken. The label in the h-maxima seed corresponding to these eight indexes is then picked. This is repeated for each pixel in a given region and each region in the centroid seeds. This allows picking up the most common label for each region in h-maxima seeds. If no correspondence is found, the neighborhood is extended to the next level. The centroid seeds with no overlap is directly transferred and combined with the rest of the h-maxima seeds and used in watershed on that frame. H-maxima seeds with no correspondence keep their original value. Additional care should be taken when this transfer of labels is performed. For example, a label of a centroid seed that is to be transferred might already be present within the h-maxima seeds. To avoid this situation, initial labeling of the h-maxima seeds is performed as starting from the highest value of the labels from the previous frame. The only consequence of this is that, if no correspondence if found, the label numbering increase fast. The check for labels also reveals when two cells merge and split and the label propagation is adjusted accordingly. For example, when two cells merge, two centroid seeds will have the same h-maxima label and in this case only one label will be propagated.

The evaluation of the method needs a "ground truth". In this case the ground truth was a sequence of cells tracked and labeled manually. A pair wise comparison is performed between a frame from the automated result and a frame from manual result. The errors are classified as over-segmentation, under-segmentation, partial detection and missing cell, see Figure 4.2. The correct segmentation rate measured as the ratio between the total number of cells tracked in the manual detection and the total number of cells that were segmented and tracked correctly is above 70%. The image sequence has comparatively low imaging frequency, every 10 minutes for 45.5 hours. The method will perform better on data sets that have cells that move rather slowly or have high imaging frequency. For cells that are rapidly moving between frames additional criteria might be needed to follow the correct track (Debeir *et al.*, 2005).

Paper II uses a variation of seeded watersheds for segmentation of cell nuclei in 3D. Smad complexes in cell nuclei are visualized by *in situ* PLA

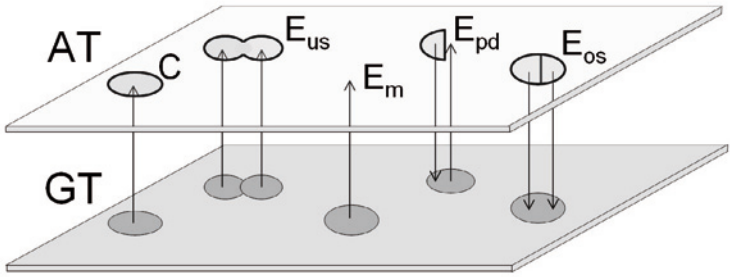

Figure 4.2: Detection of segmentation errors by pairwise comparison of automatically segmented and tracked (AT) and manually corrected ground truth (GT). A correctly segmented cell (C), and errors caused by under-segmentation (E_{us}),over-segmentation,(E_{os}),partially detected objects(E_{pd}) and missed objects(E_m).

described in Section 2.7 and imaged using confocal fluorescence microscopy. The cell nuclei are stained with Anti-Lamin-B1 and FITC. The biological observations that suggest that the kinetics of the Smad complexes and the individual Smad proteins are different and that the Smad protein activations are regulated in temporal manner were studied. The localization of the complexes thus needed to be performed in relation to the cell membrane. The emphasis here was to be able to locate the exact boundary of the cell nuclei with high accuracy in 3D.

Anisotropic smoothing discussed in Section 3.3 is used as a pre-processing step, since preserving the edge information while eliminating possible structures inside the nuclei is vital as the edge information defines splitting and merging criteria in the watershed segmentation. See Figure 4.3 for (A) original and (B) the smoothed image. As opposed to the automatic seed selection and segmentation in Paper I the nuclei segmentation is performed in a semi-automated manner where the user is allowed to select the seeds, see Figure 4.3 (D). In 3D microscopy image stacks, the attenuation of light along the z direction is present making threshold selection rather unstable unless careful measures are taken to compensate for it. The advantage with the approach in Paper II is that the input to the watershed segmentation is the 3D gradient image calculated using a 3D Sobel filter. See Figure 4.3 (C). The Sobel filter is a derivative filter that responds to edges and also takes into account the positions of the differences when approximating the gradient. This gives a more robust means to define the watershed lines. A set of linear filters are used for each direction and the results are combined to get the response at each point. The segmentation result after watershed merge is further processed by a morphological closing to obtain the final output, see Figure 4.3(G) and (H).

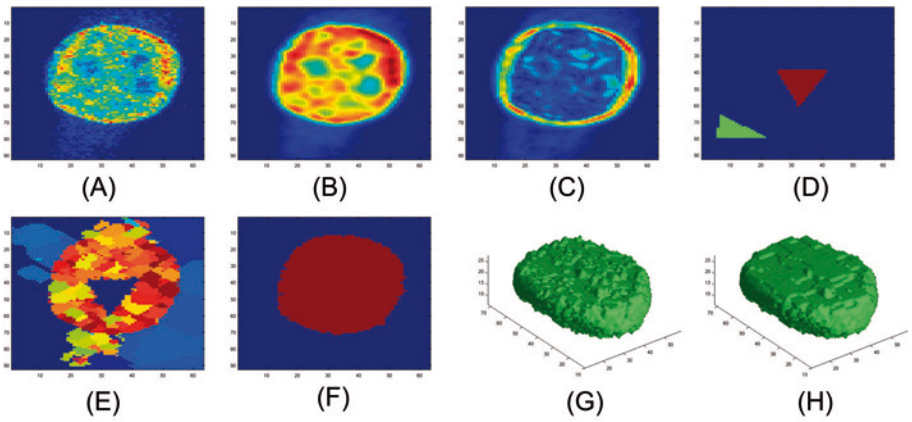

Figure 4.3: The cell nuclei segmentation process. A middle slice of (A) Pseudo-colored original image, (B) smoothed image, (C) Gradient magnitude, (D) Seeds, (E) Initial watershed result,(F) After merging to remove over-segmentation, (G) Segmented nucleus in 3D, (F) Smoothed nucleus.

In order to localize the point-like signals in relation to the nuclei membranes, a nucleus is considered as a set of shells based on the Eucliedian distance transform. The shells have negative values inside the nuclei, zero at the border and positive values outside. The outside shells are of less importance since the aim of the study is to find out what happens close to nuclear membrane. Thus the emphasis is given to the inward shells and the signal concentration is measured for each shell, see Figure 4.4. This approach gives an efficient means to calculate the signal concentration in relation to nuclear membrane. In measuring the signal concentration, we give equal importance to the distance shells independent of the size of the cell. However, there can be cells with different sizes meaning that a given distance from the nuclear membrane for a small cell would be closer to the cell center than that of a larger cell. We take the mean signal concentration at each distance from the nuclear membrane for all the cells for a given time point and this difference in "closeness" to the cell center in different cells is not visible in the final result. However, we assume that signal diffusion and movements are independent of cell size and believe that exact, rather than cell-size related measures of signal-membrane distance are more correct. In similar research work by others, automated subcellular localization is treated as a pattern classification problem (Glory and Murphy, 2007).

The watershed segmentation method has also been used as a post-processing step in the segmentation of clustered nuclei in the cytology smear images in Paper V.

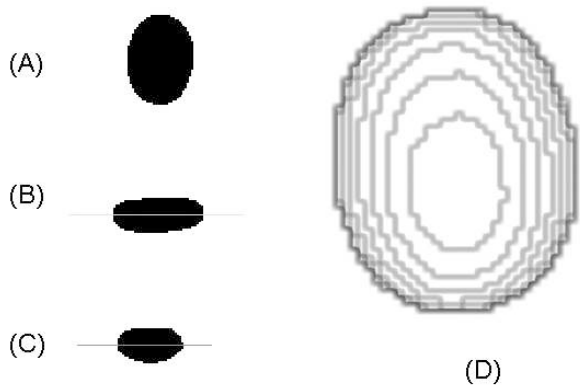

Figure 4.4: The distance shells for signal concentration measurements. (A) ,(B),(C) The segmented nucleus in xy, yz and xz views respectively. (D) The inward (negative) distance shells overlaid on the nucleus.

4.2 3D point like signal detection and localization

Paper II and Paper III

A novel method for point like signal detection is presented and its main application area is localization of protein complexes in relation to other protein complexes or subcellular compartments. As described in the previous section, Paper II is a study of localizing point-like protein signals in relation to the cell membrane. To be able to draw the biological conclusions from the data, the point-like signals need to be detected with high accuracy. A robust method should be able to separate clusters of signals and distinguish between a true signal and an intensity maxima caused by noise. An additional consideration when detecting signal localization in 3D is the point spread function of the microscope system, which typically affects the axial direction more than the lateral direction (Bolte and Cordelieres, 2006). This is also described briefly in Section 2.5.

4.2.1 Signal detection in 3D

The detection of point-like signals is performed by using a property of Fourier transform, i.e., computing the coefficients as dot products between the signal and sines and cosines (see Equation 3.2 in Section 3.2). The idea is based on a method called Stable Wave Detector (SWD) (Dupač and Hlaváč, 2006) that is used for landmark detection on 2D images. We have modified it to work in 3D, referred to as the Three Dimensional Stable Wave Detector (3DSWD). A brief description on how the method works is given below.

In the 1D case, suppose we have total data of length N, with a signal width

T/2. Then N is divided into n overlapping frames i=1...n with length T. The frames should overlap more than T/2. Sine and cosine Fourier coefficients, b_i and a_i, of the first harmonic wave of the Fourier series are computed using

$$\begin{aligned} a_i &= F_i C \\ b_i &= F_i S \\ C(t) &= cos(2\pi(t/T)) \\ S(t) &= sin(2\pi(t/T)) \end{aligned} \tag{4.1}$$

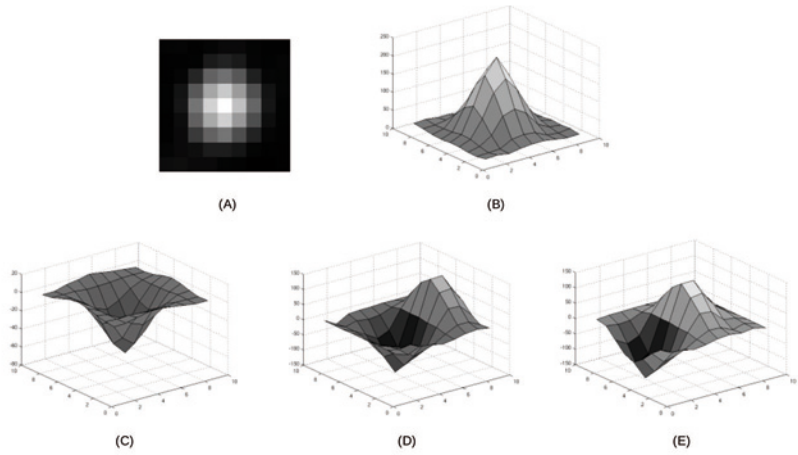

Figure 4.5: Point-like signal detection and verification using sine and cosine filters. (A) The mid slice of a simulated point-like signal, (B) The signal as a surface plot. (C) Cosine filtered output, sine filtered output in x direction in frame before (D) and frame after (E).

Where F_i is the intensity data of frame i, and C and S are discrete cosine and sine functions with period T and t=0...T-1. In general a frame containing a signal will have a negative cosine coefficient ($a_i < |b_i|$) and be surrounded by one rising and one falling edge, i.e., a negative sine (b_i<0) and a positive sine (b_i>0).

The 3DSWD contains some modifications of the original SWD based on our observations on image data. The signals of interest are often small and may be close to each other in space. Therefore, we let the frames overlap by T-1, resulting in a regular convolution of the image with a cosine and sine function. The cosine filtration works as the detector of the possible signals. In order to make filters symmetric around a center point, value t for the cosine filters is set to 0...T, where T is an even number. The sine function works as the verifier/separator. The period for the sine function is set to half of the period of cosine to increase the resolution detection of closely lying signals. As a

result, the frames of the sine function are set to half the size of the frames of the cosine function. See Figure 4.5 for the filter responses on a 2D slice of a point-like signal.

The filter design in 3D needs some additional considerations. The cosine filter is built up by combining three 1D cosine functions for all three directions x, y and z into a 3D filter. Due to PSF of the signal the period in the axial direction is made longer than in the lateral direction using the ratio of axial to lateral frequency. The sine filter works as a derivative filter describing the gradient in the image. It is important to get the orientation of the gradient in all directions and hence it is not possible to combine the three 1D filters into a single 3D filter. Instead three 1D filters are used in each direction. In order to increase the specificity of the method, the diagonal directions can also be used.

The method is applied to images and signals are detected as follows. The image is first convolved with the cosine filter C of period T and a threshold is used to identify the potential signals. Next, the image is convolved with the three different sine filters . In order for a pixel to be classified as a true signal, rising and falling edge checking criteria mentioned above, is used for each direction x,y and z.See Figure 4.6(A) for a snapshot of a 3D visualization of detected PLA signals from image data in Paper II.

4.2.2 Performance evaluation

In Paper II, the point-like signal detection method was briefly evaluated for its performance in relation to other methods that have been studied, as can be seen in Figure 4.6. The comparison is performed with three other methods, the difference of Gaussian (DoG) (Sonka *et al.*, 2007), the Tophat transformation (Vermolen *et al.*, 2005) and the use of Hessian matrix (Lindeberg, 2000). The DoG is obtained by subtracting a wide Gaussian from a narrow Gaussian. The Tophat method makes use of the difference between morphological opening, and the original image. Hessian matrix, the matrix of second order partial derivatives is used to obtain the eigen values to detect point-like signals.(Sato *et al.*, 2000). Figure 4.6(B) shows a 2D slice form the simulated signal volume. Figure 4.6(C) shows the plots of the percentage of true signals detected by each of the methods (solid lines). The dashed lines are the amount of false positive allowed for each method by setting a threshold. This result shows a better performance of the 3DSWD.

Paper III is an extensive study on the point-like signal detection method presented in Paper II in order to evaluate its performance. The motivation for this study were the issues that had to be dealt with such as the noise levels, signal strength and size and the closely lying signals in image data used in Paper II. The performance is evaluated in a number of experiments using both artificial image data and microscopy image data. Three other methods that we found were used in recent research of similar type of signal detections

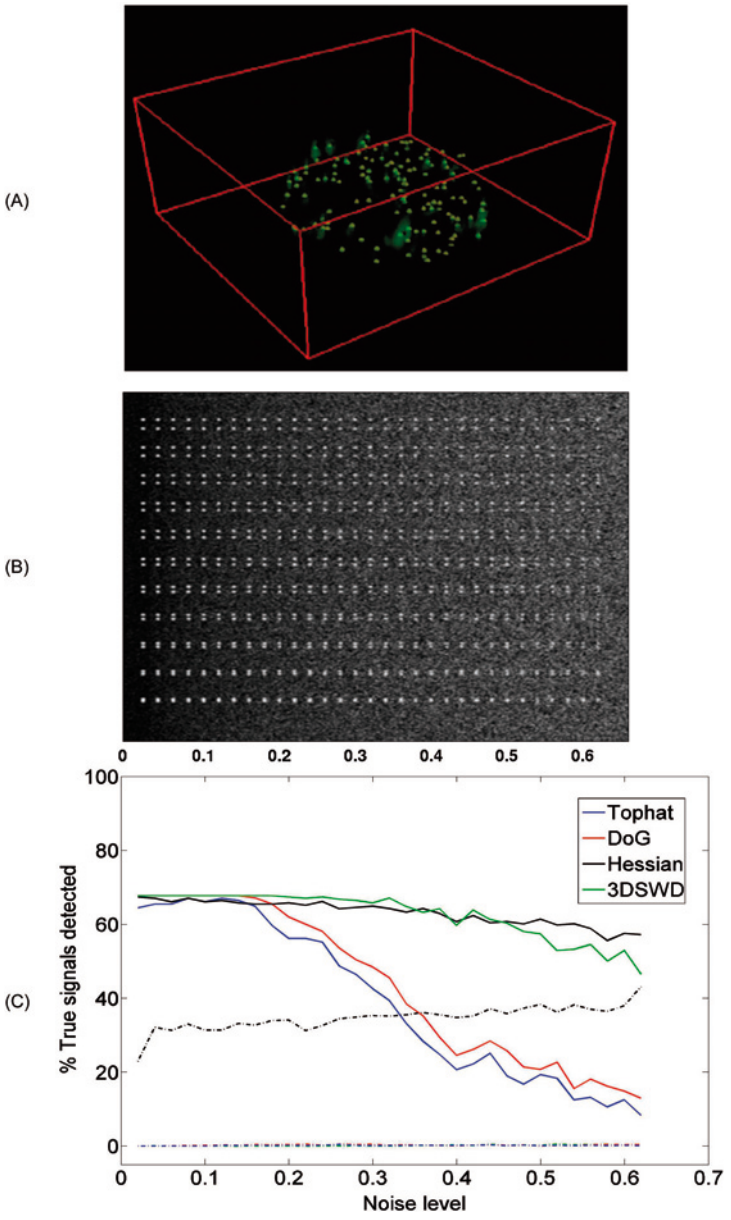

Figure 4.6: Point-like signal detection results and method comparison. (A) A snapshot from a 3D visualization of the detected PLA signals (in green) using 3DSWD (yellow markers). (B) A 2D slice from the simulated signal volume with signals with increasing noise level (left to right) and increasing closeness (top to bottom). (C) The plot of the percentage of signals detected by the 3DSWD and three other methods used for comparison, namely the TopHat transform, Difference of Gaussian (DoG) and the Hessian method. The percentage of false positives were kept at the same level (dashed lines) except for Hessian that had highest sensitivity to noise.

in 3D namely the TopHat transform (Vermolen *et al.*, 2005), that was used in Paper II as well, a multi-resolution approach (Vermolen *et al.*, 2008) and the DoG (Difference of Gaussian) (Kruizinga and Petkov, 2000) have been used in the comparison. The testing involved simulating the signals, type of noise available and the closeness of signals in order to test the performance of the method. The tests performed on this type of simulated data as well as actual image data reveals the methods better performance in robustness to noise, resolving power and sensitivity to signal intensity. See Figure 4.7 for one example where the resolving power and sensitivity to signal intensity is evaluated for 3DSWD and the other three methods. Signals of different sizes are commonly seen in real images. The 3DSWD targets one size of signals but can be used in a loop over a range of values of T to find signals of different sizes.

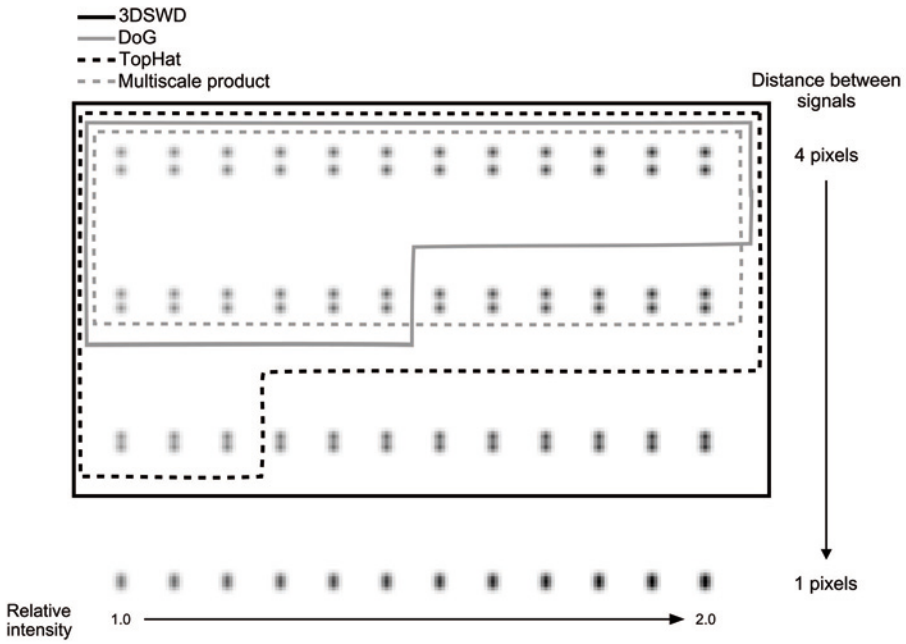

Figure 4.7: Resolving power and sensitivity to signal intensity. Regions inside the lines contain signal pairs that have been correctly detected. Outside the region a single signal was detected for each pair of signals. The regions represent the detected pairs of signals when the maximum number of signals in the image has been detected by each method.

4.3 Cell confluence measurements for time-lapse microscopy

Paper IV

An automatic method for quantifying cell confluence of a time sequence of fibroblasts, imaged using phase contrast microscopy is presented. The method uses wavelet based texture features, to classify the images into regions consisting of interphase cells and proliferating and/or necrotic cells. The images are positive phase contrast images obtained using an inverted microscope with phase contrast.The wavelets are briefly described in Section 3.6.2. The extension to complex wavelets and result obtained from the more directional oriented real-oriented DT-CWT is also shown (see Figure 3.8). In Paper IV, we use the real oriented DT-CWT to obtain parameters for classification of cells in culture.

The sub-bands of the real oriented DT-CWT represent the texture in such a way that the elongated shape of interphase cells can be distinguished from the more rounded proliferating and/or necrotic cells. Figure 4.8 shows this using a single interphase cell (A) and a proliferating cell (B) as test images. The two images are decompose into first level real-oriented DT-CWT subbands. For each of the directional subbands the GLCM property Energy, which is the sum of squared elements of the GLCM , is obtained. Figure 4.8(C) shows the two energy plots corresponding to the two images. The elongated interphase cell has a given orientation that contributes to one or a few of the six oriented wavelet sub-bands, while the round proliferating cell contributes more or less equally to all six sub-bands. Hence, the difference between the maximum and minimum energy can be used to classify the regions.The images are classified not as individual cells, but as small regions consisting of the cells. To speed up the classification step, the images are first divided into smaller regions of 32x32 using quad tree decomposition (QTD). The regions found to be uniform are set as background during this step. Features from the wavelet sub-bands of these regions are used for classification of the regions as containing interphase cells, proliferating and/or necrotic cells, and background.

A confluence measure as well as a measure of proliferating and/or necrotic cells is extracted for each new image of a time sequence, see Figure 4.9. This monitoring of cell growth provides a means for direct harvest of confluent cells and a system for warning if the proportion of proliferating and/or necrotic cells becomes exceptionally high. The proposed method is also tested for robustness to variations in microscopic settings such as different focus levels and lighting conditions. The method is stable for different lighting conditions and this is due to the fact that the texture measures actually are related to the shape (round proliferating cells and long interphase cells) as opposed to other texture measures that might differ under different light settings. Out-of-focus

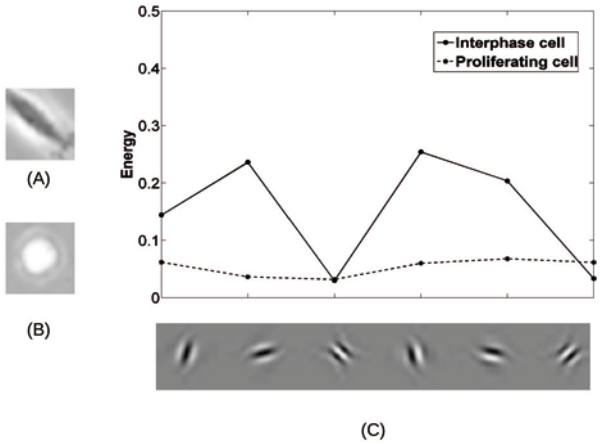

Figure 4.8: The energy response from each of the different oriented sub-bands of the real-oriented DT-CWT applied on a sub-region of 32x32 pixels containing an elongated interphase cell and a sub-region containing a rounded, proliferating cell.

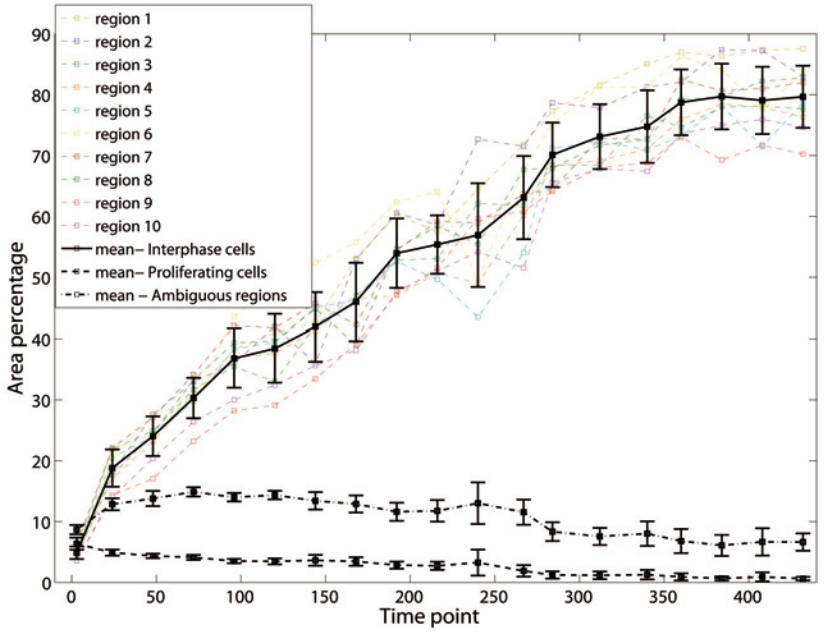

Figure 4.9: The increase in confluence over time. The error bars represent the standard deviation. The plot shows the mean cells confluence measure (solid curve) over time together with the individual curves in color for each region. The plot indicates an early, rapid increase of cell numbers, followed by a more constant number of cells after confluence is reached. The plot also shows the area percentage of proliferating cell regions (dashed curve) and the ambiguous regions (dot-dash curve). The values shown here are the mean of the values of the 10 different regions.

images have a greater negative effect on the measurements. This can also be seen by the outliers in the individual curves of Figure 4.9. These were caused by few de-focused images in the image sets and we believe that the best way to solve this is to incorporate an auto-focus method into the automated system to select the best focus level (Kozubek *et al.*, 2001), discussed also in Section 2.1.

4.4 Pre study of color spaces for cytology

Paper IV

Digital image analysis has become an indispensable tool in cytology since the normal visual inspection of diagnostic procedures could be partially or completely replaced with automated methods in order to get less error prone results (Bengtsson, 2003). Paper V is an initial study of the ability to use color information on digital images for applications in cytology. Fine needle aspiration cytology smears of thyroid lesions stained with the Papanicolau stain were used in this study. By using the correct color space and further methods to deal with clustered nuclei, the method can be used to assist the pathologists who, at present are inspecting the sample visually to identify the malignancies. The patients from whom the samples that are classified as being malignant are extracted are then subjected to a surgical excision to obtain a histological sample. The number of surgical excisions required can be reduced if more effective methods are incorporated in the initial diagnosis. In addition, the already obtained pairs of cytological and histological samples can be used as a means for evaluating the method. Figure 4.10 shows what a typical color image obtained with Pap staining would looks like. The images can come with varying levels of clarity as can be seen. (A fact worth mentioning is that the way these patient samples are handled prevented us from being involved in image acquisition process.) There are various quantitative parameters such as nuclear size, cell size, nuclear shape, nuclear-to-cytoplasmic ratio and cell shape that can be used to detect a malignancy using these smear samples (Ramesh *et al.*, 1998). Among these, the nuclear size is a major factor which enables the detection of malignant cells. This means the digital image analysis task is to correctly segment the nuclei and extract one or more of these parameters. The aim of this study was to see the effect of using different color spaces and using color information for this task. The fact that in addition to providing better contrast, the color information available on these images provides additional information about the malignancy is taken in to consideration when deciding to perform the analysis on color images rather than the gray scale. The obvious question then is about what the best representation of color would be. A number of choices have been tested in this study. The RGB and HSV color spaces described in Section 3.5 are used in addition to two other methods, namely a principle component analysis (PCA) based color space and a color

space fusion (CSF) method. Use of PCA based color space is described in detail in (Ranefall 1998). The PCA is applied to the original RGB image and the three principle components are used. The CSF described in (Lezoray *et al.*, 2003) is a method that makes use of two color spaces, RBG and CIE_{Luv}. The difference between the blue and green components in RGB is combined with the v component of Luv and normalized to obtain a binary image that segments the nuclei.

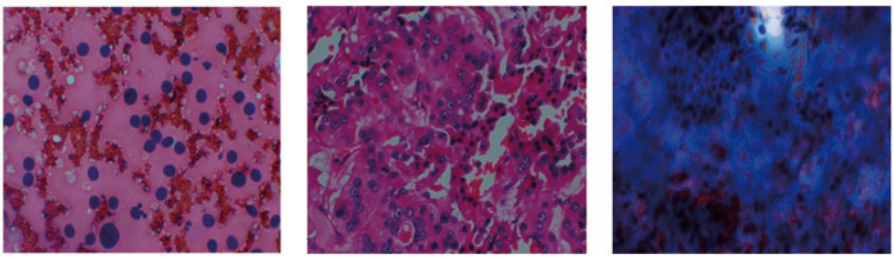

Figure 4.10: Pap stained thyroid smear images (nuclear stain haematoxylin (blue) and cytoplasm staining eosin (pink/red)). (A), (B) and (C) show the how much variation in the image quality is present between different images.

For HSV, PCA and RGB color spaces, the average color to be segmented is calculated using a user selected mask. The distance to this mean color vector in the color space from each of the pixels in the image is calculated. As a selection criteria of similarity between the mean and each of the other pixels, a threshold value which is the standard deviation (SD) of the sample, i.e., the average distance from the mean to a data point in the sample was used. The distance measure is taken either as Euclidean or the generalized Mahalanobis distance that uses the covariance matrix of the selected sample representing the color of interest. If the segmentation based on this initial threshold is not satisfactory, a multiple of the initial value of the SD can be used until the result becomes satisfactory. A size thresholding which remove the small objects was applied to the results.

The visual inspections of the results obtained for the different color spaces that have been tested revealed that the best results are obtained using RGB color space despite its known drawbacks. This result agrees with that of (Lezoray *et al.*, 2003) where they use a color space choice measure on similar type of images. The detailed analysis of feature extraction and interpreting the results using corresponding histological samples have not yet been addressed.

5. Conclusions and future work

An important aspect deciding future work is the fact that the knowledge gained throughout the postgraduate study period needs to be used mainly in educating possible future researchers in the field of applied digital image processing. The aim of gaining such competence in the field of digital image processing, as the author sees, has successfully been achieved. When it comes to future work on research, there are number of continuations that could be carried out related to the work presented in this thesis. In addition, the author is expected to take part in building strong research groups within her working environment at University of Peradeniya, Sri Lanka, which is one of the main aims of the project that funded the studies. This is a rather challenging aim since it means initiating collaborations with researchers in biology and medicine. A step towards this goal has already been taken with the work in Paper V and this will be part of the aimed future work as stated below.

In the cell tracking application of Paper I the tracking algorithm can be associated with the actual cell characteristics, e.g., the fact that cells become fairly circular close to division, in order to improve the tracking of merging and splitting cells. Additional criteria are also needed to handle the cells that disappear and re-appear close to the image border. Cells that disappear into clusters also causes problems as heavy clustering often occurs in this type of cell cultures.

The biological conclusions that are expected to be drawn from the results in Paper II need further testing on, e.g., other proteins that interact with Smad complexes. Larger data sets are needed to compensate for cell to cell variations.

The real image data from mitosis research used in evaluating the 3DSWD method in Paper III is yet to be analyzed. The main aim is to study how the PLA signals colocate with the kinetochore markers and some initial testing has shown promising results that need to be further investigated.

To use the benefit of the results of Paper IV, the method needs to be incorporated with the automated system. This requires further refinements of to the method, as the method was developed with producing successful results in mind, rather than having an optimized implementation that can be used directly. This will need better understanding of how the system works and better auto-focusing is needed for the method to work efficiently.

The initial study on color spaces for cytology in Paper V is an important part in future research. The image data were obtained from the Department

of Pathology at University of Peradeniya, Sri Lanka, a part of the University the author is employed at. The samples come from patients at the University Teaching Hospital and they are smears of thyroid nodules, a common origin of malignancy in Sri Lanka. Around 100 such samples arrive at the Pathology Department each day and the present examinations on malignancies in them are performed manually by a pathologist who sits at the microscope and examines each sample. Needless to repeat the often mentioned drawbacks of such approaches, the aim of initiating the work related to Paper V is to develop a system that can assist the pathologist in the diagnosis process. Correctly diagnosed patients with malignancies will undergo a surgical excision procedure and thus the initial smears will be accompanied by a corresponding histological sample as well. The long term goal is to cross validate them and to have a database so that the new samples that arrive can be diagnosed fast with high accuracy.

In conclusion, it should be pointed out that we cannot solve problems by using the same kind of thinking we used when we created them (Albert Einstein, 1879-1955). Thus, there will be more questions to be answered when the future work mentioned above is actually carried out, hopefully contributing positively to the field.

6. Brief summary of Papers

This thesis presents digital image analysis methods in 2D, 3D and time, for different applications in cell biology. Three types of microscopy, bright field, phase contrast and confocal fluorescence microscopy have been used in acquiring image data. In **Paper I**, cell migration analysis is the focus and the time lapse bright field image sequences were obtained from a project with main concern on investigating the mechanisms behind differentiation of neural stem/progenitor cells. Combined tracking and segmentation is performed by seeded watersheds and the results coincide with those obtained from manual tracking. The method has the advantage of being able to perform both segmentation and tracking simultaneously.

Paper II deals with localization of point-like signals on 3D confocal fluorescent microscopy images. The signals are those that detect Smad complexes within cell nuclei using the proximity ligation assay (PLA). Smad proteins are transcription factors and the subnuclear localization of them defines their function. Thus the aim is to detect the signals with high precision and also to localize them in relation to nuclear membrane. The results from the method regarding signal localization and concentration agree with biological observations that suggest that the activation or repression of transcriptions is regulated in a temporal manner. Further studies are needed in order to fully understand the behavior of the complexes.

The 3D point-like signal detection method that proved to give robust results in Paper II has been further investigated and improved in **Paper III**. The intention is to evaluate the method in detail for its robustness to noise, resolving power and sensitivity to signal strength and also to compare it with other commonly used point-like signal detection methods. With results obtained on simulated data, the method shows promising performance and gives significantly better results compared to other methods. The tests performed on real image data from mitosis research proves further the ability of the method to be used as a tool in signal detection and localization application in 3D.

Time lapse microscopy image sequences are not only used for cell migration analysis. They can also be used in other applications such as tissue culture where the culture are either simple expansion of cells for research purposes or they are part of a tissue engineering process that result in implants that can be used on patients. In such cases it is important to monitor the culture over time for possible necrosis and also to decide when

the culture has reached confluence. **Paper IV** is a study on such time lapse sequence of fibroblasts images under phase contrast microscopy. The images are classified based on texture using wavelets and hence provide a means not only to measure confluence but also to detect necrosis. The method is also stable for different lighting conditions of the microscope and the results on the cell confluence measurements agree with actual observations.

Quantitative measurements on cell nuclei are an important part of both cytological and histological examinations when detecting malignancies. Papanicolau, more commonly known as Pap, staining is a key element in many of these types of studies. The color information given by the stains not only is useful for increasing contrast in the images, but can also be incorporated in the diagnosis procedure. **Paper V** is an initial study with this aim, i.e., studying the applicability of information from different color spaces for in the diagnosis process. This study is expected to be continued so that the results from the most successful method can be compared with the corresponding surgical excision of the histological samples.

7. Summary in Swedish

I den här avhandlingen presenteras metoder för analys av bilder av celler. Bilderna är digitala, insamlade med olika ljusmikroskopitekniker. Ljusmikroskopi som teknik är väl etablerad inom biologisk och medicinsk forskning. Bilderna som skapas kan vara tvådimensionella (2D), tredimensionella (3D), eller sekvenser av bilder tagna vid olika tidpunkter. En digital 2D bild representeras som en matris, där varje element i matrisen kallas "pixel"; en förkortning av engelskans "picture element". I en svartvit bild har varje pixel ett värde som motsvarar ljusheten, eller intensiteten. I färgbilder representeras färgen hos en pixel med tre intensitetsvärden; ett för rött (R), ett för grönt (G), och ett för blått (B). En 3D bild representeras ofta som en mängd 2D bilder staplade ovanpå varandra. De olika 2D bilderna är tagna vid olika fokalplan i mikroskopet, och varje bildelement kall as "voxel". Om en sekvens av bilder samlas in blir tiden en ytterligare dimension. De bildanalysmetoder som presenteras i den här avhandlingen är tillämpade på 2D bilder, 3D bilder, och sekvenser av bilder, som alla visar olika typer av celler.

Stamceller är en typ av celler som ännu inte är fullt differentierade, dvs. de kan fortfarande utvecklas till olika typer av celler, som t.ex. neuroner. Ett sätt att studera mekanismerna bakom differentieringen är att följa cellerna över tiden. När man ska analysera en sekvens av bilder måste man både segmentera, dvs. separera objekt från varandra och från bakgrunden, och följa objekten över tiden. Vattendelar-"Watershed" segmentering är en populär metod för bildsegmentering som delar upp bilden beroende på intensiteten hos bildens pixlar. Bilden betraktas som ett landskap, som sakta översvämmas av vatten som tränger upp från alla lokala minima, eller dalar, i landskapet. När två vattenmassor möts byggs en dam, dvs. en vattendelare. Till slut är bilden uppdelad i en mängd regioner avgränsade av dammar. Genom att använda fördefinierade startpunkter, eller frön, kan segmenteringen göras mer specifik. Här presenteras en vattendelar–baserad metod för att både segmentera och följa stamceller över tiden. Då både cellernas mitt och bakgrunden har liknande intensitetsfördelning behövs frön. Bakgrundsfrön definieras baserat på den lokala variansen i bilden, då bildbakgrunden har lägre lokal varians än cellerna. Objektfrön definieras initialt som lokala maxima av en given storlek (med hjälp av h-maxima transformen). Objektetiketterna från den initiala segmenteringen förs sedan

vidare till nästa bild i tidsserien, och jämförs med nya h-maxima. Varje nytt h-maximum som hittas tilldelas den objektetiketter med vilken den har störst överlapp. Med denna metod kan man också hantera celler som delar sig. En delande cell har t.ex. en objektetikett i bilden före celldelningen, och två etiketter efteråt; den ena av de nya cellerna behåller etiketten, medan den andra får en ny. Den här metoden att följa celler är enkel och effektiv, och resultatet stämmer överens med resultat från manuella/visuella metoder så länge cellerna inte klumpar ihop sig i täta kluster.

Med hjälp av fluorescensfärgning kan olika cellkomponenter märkas in och detekteras på ett selektivt sätt. Proteiner och proteinkomplex kan detekteras med mycket hög specificitet. Transforming Growth Factor (TGF) beta är en stor proteinfamilj som kontrollerar en rad cellfunktioner, så som t.ex. celldelning. Smad i sin tur är en grupp av proteiner som reglerar aktiviteten av TGF-beta. Smad-proteinerna bildar komplex som kan detekteras med hjälp av proximitetsligering (Proximity Ligation Assay, PLA). Genom att studera var olika Smad-komplex befinner sig i relation till cellkärnans membran vid olika tidpunkter kan man få fram information om funktionen hos Smad-komplexen. För att göra det måste först cellkärnans membran segmenteras fram från en 3D bild skapad med hjälp av konfokalmikroskopi. Här presenteras en vattendelar–baserad metod som utnyttjar objekt- och bakgrundsfrön i kombination med bildgradienten. Gradientens magnitud är stor vid cellkärnans kant, vilket gör att kärnans membran kan hittas med hög noggrannhet. Fluorescens signalerna från de PLA-detekterade Smad-komplexen är små och punktformade. De detekteras med en metod baserad på Fouriertransformen, vilket innebär att metoden utnyttjar en frekvensbaserad representation av bilden. Filter som detekterar och verifierar detekterade signaler byggs upp utifrån en diskret representation av Fouriertransformen. De detekterade signalernas position i relation till cellkärnans membran beskrivs sedan med hjälp av Euklidiska avståndsmått. Resultaten stämmer överens med observationer som gjorts med hjälp av andra, icke bildbaserade metoder, men fler studier behövs för att verkligen förstå Smad-komplexens funktion.

Den metod för detektion av punktformade signaler som nämns ovan är användbar för en mängd andra bildanalysapplikationer, och har därför utvärderats mer i detalj. Olika bilder kan ha olika brusnivå, och signaler kan vara olika ljusstarka samt ligga mer eller mindre nära varandra. Vi har därför utvärderat metodens bruskänslighet, känslighet för signalintensitet, samt förmåga att upplösa närliggande signaler. Prestanda har jämförts med tre andra välkända metoder för signaldetektion, och vår nya metod är bättre på att detektera signaler som ligger nära varandra i brusiga bilder.

Genom att odla celler kan man få en större mängd celler av samma sort. Cellodling används också för att skapa nya vävnader som kan användas som implantat i patienter. Genom att övervaka cellodlingen kan man avgöra när odlingsytan är täckt av celler, och det är dags för skörd. Wavelets är en bildrepresentation som bygger både på frekvens och rumslig position.Här visar vi hur Wavelets kan användas för att beräkna celltätheten i en serie av bilder av odlade celler tagna vid olika tidpunkter. Wavelettransformen gör om originalbilden till ett antal nya bilder, eller sub-band, som beskriver horisontell, vertikal, och diagonal bildinformation för en given skala. Man kan på så sätt finna texturegenskaper av en given storlek. Den Wavelettransform som använts här mäter texturegenskaper i sex olika riktningar, och kan särskilja mellan långsmala, växande celler, och runda, delande celler. Bilden delas in i flera små regioner, och energin hos sub-banden används för klassificering. De långsmala cellerna har hög energi i en dominerande riktning medan de runda cellerna har ungefär samma energi i alla riktningar. Den resulterande klassificeringen överensstämmer med den observerade celltätheten och är stabil vid varierande mikroskopinställningar. Då även döende celler är runda i formen kan metoden ge information om cellodlingens hälsa genom att beräkna förändringar i andelen runda celler.

Kvantitativa mätningar på celler är viktiga både för cytologi, dvs. läran om celler, och histologi, läran om vävnaders uppbyggnad, och därtill relaterade sjukdomar. Papanicolaou-, eller Pap-färgning är en vanligt förekommande färgningsmetod. Färgen skiljer sig mellan cellkärnorna och cellernas cytoplasma, och färginformationen kan användas för att segmentera fram cellkärnorna för att sedan extrahera olika kvantitativa mått. Vi har studerat hur färginformationen i en serie bilder av Pap-färgade sköldkörtelpreparat kan användas. Olika färgrymder, utöver den vanliga RGB-representationen, har utvärderats, men resultaten visar att den mest korrekta kärnsegmenteringen fås om RGB-rymden används, vilket också stämmer väl överens med tidigare studier av liknande bilddata.

De metoder som presenteras i denna avhandling är användbara verktyg för analys av 2D, 3D och tids serier, och kan används även inom andra tillämpningsområden.

8. Acknowledgments

This thesis summarizes the work carried out at Centre for Image Analysis, Uppsala University Sweden and University of Peradeniya, Sri Lanka, during the period from September 2004 to January 2009. I express my gratitude to all the people who made it possible by contributing in one way or the other. Special thanks go to following people;

- My supervisor, Assistant Prof. Carolina Wählby, who is much more than just a supervisor. Thank you for your constant support, good advices not only on research but on many other things as well. Most of all, thank you for your friendship and the thoughtfulness that you always show.
- Prof. Ewert Bengtsson, my assistant supervisor and the head of CBA, first of all, for opening the doors of CBA to me and making me feel welcome, always. Thank you for supporting me in every possible way.
- Dr. Mahinda Alahakoon my local supervisor, for helping me keep focused during the time spent in Sri Lanka and also taking care of equipment purchase etc. to help me perform my work.
- The funding agency SIDA and everyone involved in the funding program are gratefully acknowledged. Late Prof V.K. Samaranayake(UCSC) who initiated the program is specially mentioned. Prof. Richard Wait, the coordinator at Uppsala University is also acknowledged.
- Lena Wadelius, for taking care of EVERYTHING and making CBA a nice place to be at.
- Olle Eriksson for keeping the systems at CBA running smoothly and all the help with computer related issues.
- Everyone else, old and new, senior and junior, who contribute/contributed to the "friendly CBA" environment; Ewert, Gunilla (thank you also for advices on correct English), Ingela, Olle , Tommy, Bosse, Ingrid, Joakim, Stina, Carolina, Cris, Anders H, Anders B, Stefan, Ida , Caterine , Robin, Fredrik , Nataša, Mats, Ola, Pasha, Lucia, Maria, Erik V, Patrick, Magnus, Milan (my nice office mate), Amin, Filip, Kristin, Hamid, Khalid, Gustaf, Patrik , Erik W., Bettina, Lennart, and Hyun Ju.
- All my co-authors and collaborators, mainly Amin , Agata, Katerina, Dr. Ratnatunga, Hans, Mariaana and Marko, it was nice working with you.
- Everyone who helped in proofreading this thesis, Ewert, Lina, Ingela , Gunilla and Hyun Ju.

- Larry Graup, production editor of Cytometry, thank you for answering my many email requests promptly, and sending the nice high resolution version of Paper III, within just few hours of my request.
- Ulrika Andersson at IT department, for helping in many things and friendship.
- Carolina's nice family; Anders and kids, and Sven and Carola, I am glad that I met you all and thank you for the good times together. Let's hope that one day you could visit us in Sri Lanka.
- The family of Jos and Elles ; thank you for welcoming us warmly, to your beautiful home, good advices and friendship. Uppsala became a much nicer place, because of you.
- Lars, Margerita and Rebecca, for being the nicest of landlords and being helpful in many ways.
- All my Sri Lankan friends. Thank you for being the "family" in Uppsala for us.
- My fellow PhD candidates from Sri Lanka , thank you for friendship.
- My other friends in Uppsala, for friendship and happy times together.
- My very best friends, the group of 13, though we are not together anymore, it is always nice to know that I could turn to any of you for anything, anytime. Thank you for helping me to keep my spirit high during the long working days.
- Staff and colleagues at Department of Statistics and Computer Science for all the help, looking forward to start working with you again.
- Everyone in my family, my parents, for your endless love and care, for always believing in me and being there and for giving me courage and strength to pursue my dreams.
- My two sisters and their families and my extended family; I am lucky to have you all in my life. Thank you for being there for me, always.
- The most important two persons, my husband Jeevan , for all the love and happiness you give me, for your patience, for keeping your career goals aside for a while (a long while) to help me achieve mine, for taking care of and everything. Without you, this would never have been possible.
- My dear little son Seniru, for the endless inspiration and giving a whole new meaning to my life. The long hours of work, were always paid off, with just one smile from you!

Thank you all!

අමල්කා පීනිදියආරච්චි .

Uppsala, January 2009

Bibliography

[1] Abella M., Zubeldia J.M., Conejero L., Malpica N., Vaquero J.J., and Desco M. Automatic quantification of histological studies in allergic asthma. *Cytometry Part A*, 2008. Early View. DOI: 10.1002/cyto.a.20648.

[2] Alberts B., Johnson A., Lewis J., Raff M., Roberts K., and Walter P. *Molecular Biology of the Cell*. Garland Publishing Inc. Chapter 9, 4th edition, 2002.

[3] Althoff K. *Segmentation and tracking algorithms for in vitro cell migration analysis*. PhD thesis, Chalmers University of Technology, Göteborg , Sweden, 2005.

[4] Arivazhagan S. and Ganesan L. Texture classification using wavelet transform. *Pattern Recognition Letters*, 24(9):1513–1521, 2000.

[5] Bengtsson E. Computerized cell image analysis: past present, and future. *Lecture Notes in Computer Science, Springer, Berlin*, 2749:395–407, 2003.

[6] Beucher S. and Lantuéjoul C. Use of watersheds in contour detection. *International Workshop on Image Processing. Real-time and Motion Detection/Estimation, Rennes, France*, 1979.

[7] Bolte S. and Cordelieres F. P. A guided tour into subcellular colocalization analysis in light microscopy. *Journal of Microscopy*, 224(3):213–232, 2006.

[8] Brenner J., Dew B.S., Horton J.B., King T., Neurath P.W., and Selles W.D. An automated microscope for cytologic research - a preliminary evaluation. *Journal of Histochemistry and Cytochemistry*, 24(1):100–111, 1976.

[9] Cantrill S. Nobel prize 2008: Green fluorescent protein. *Nature Chemistry*, 2008. doi:10.1038/nchem.75.

[10] Chang T. and Kuo C.-C. J. Texture analysis and classification with tree-structured wavelet transform. *IEEE Transactions on Image Processing*, 2(4):429–441, 1993.

[11] Cheng H.D., Jiang X.H., Sun Y., and Wang J. Color image segmentation: advances and prospects. *Pattern Recognition*, 34(12):2259–2281, 2001.

[12] Davidson M.W and Abramowitz M. Optical microscopy. http://www.olympusmicro.com/ primer/microscopy.pdf, November 2008.

[13] De Hauwer C., Darro F., Camby I., Kiss R., Van Ham P., and Decaesteker C. In vitro motility evaluation of aggregated cancer cells by means of automatic image processing. *Cytometry*, 36:1–10, 2005.

[14] Debeir O., VanHam P., Kiss R., and Decaestecker C. Tracking of migrating cells under phase-contrast video microscopy with combined mean-shift processes. *IEEE Transactions on Medical Imaging*, 24(6):697–711, 2005.

[15] Degerman J. *Time lapse bight-field microscopy and image acquisition of in-vitro neural stem cells*. Licentiate thesis, Chalmers University of Technology, Göteborg, Sweden, 2007.

[16] Dupač J. and Hlaváč V. Stable wave detector of blobs in images. *Proceedings of 28th Annual Symposium of the German Association for Pattern Recognition, Berlin, Germany, Springer Verlag LNCS 4174*, pages 760–769, 2006.

[17] Glory E. and Murphy R.F. Automated subcellular location determination and high throughput microscopy. *Developmental Cell*, 12:7–16, 2007.

[18] Haralick R.M, Shanmugan K., and Dinstein I. Textural features for image classification. *IEEE Transactions on Systems, Man and Cybernatics*, 3(6):610–621, 1973.

[19] Hatipoglu S., Mitra S. K., and Kingsbury N.G. Texture classification using dual-tree complex wavelet transform. *Proceedings of the 7th International IEEE Conference on Image Processing and Its Applications, Manchester, England.*, pages 344–347, 1999.

[20] Kim T-Y., Choi H-J., and Choi H-K. Cell nuclei image classification using three-dimensional texture features. *HEALTHCOM 2006. 8th International Conference on e-Health Networking, Applications and Services, New Delhi, India*, 2006.

[21] Kingsbury N.G. The dual-tree complex wavelet transform: a new efficient tool for image restoration and enhancement. *In proceedings of the 9th European Signal Processing Conference (EUSIPCO 98)*, 1998.

[22] Kingsbury N.G. Complex wavelets for shift invariant analysis and filtering of signals. *Applied and Computational Harmonic Analysis*, 10(3):234–253, 2001.

[23] Klar T. A., Engel E., and Hell S. W. Breaking abbe's diffraction resolution limit in fluorescence microscopy with stimulated emission depletion beams of various shapes. *Physical Review*, 64(066613):066611–066619, 2001.

[24] Kozubek M., Kozubek S., Lukáscaronová E., Bártová E., Skalníková M., Matula Pa., Matula Pe., Jirsová P., Cafourková A., and Koutná I. Combined confocal and wide-field high-resolution cytometry of fluorescent in situ hybridization-stained cells. *Cytometry*, 45(1):1–12, 2001.

[25] Kruizinga P. and Petkov N. Computational model of dotpattern selective cells. *Biological Cybernetics*, 83(4):313–325, 2000.

[26] Lezoray O., Elmoataz A., and Cardot H. A color object recognition scheme: application to cellular sorting. *Machine Vision and Applications*, 14(3):166–171, 2003.

[27] Lindeberg T. Detecting salient blob-like image structures and their scales with a scale-space primal sketch: A method for focus-of-attention. *International Journal of Computer Vision*, 11(3):283–318, 1993.

[28] Lindblad J., Wählby C., Bengtsson E., and Zaltsman A. Image analysis for automatic segmentation of cytoplasms and classification of rac1 activation. *Cytometry Part A*, 57A(1):22–33, 2004.

[29] Meijering E., Smal I., Dzyubachyk O., and Olivo-Marin J-C. *Microscope Image Processing-Time-Lapse Imaging, Q. Wu, F. A. Merchant, K. R. Castleman eds.* Elsevier Academic Press, 2008.

[30] Ojala T., Pietikäinen M., and Harwood D. A comparative study of texture measures with classification based feature distributions. *Pattern Recognition*, 29(1):51–59, 1996.

[31] Ojala T. and Pietikäinen M. Unsupervised texture segmentation using feature distributions. *Pattern Recognition*, 32:477–486, 1999.

[32] Otsu N. A threshold selection method from gray-level histograms. *IEEE Transactions on Systems, Man, and Cybernetics*, 9(1):62–66, 1979.

[33] Perona P. and Malik J. Scale-space and edge detection using anisotropic diffusion. *IEEE Transactions on Pattern Analysis and Machine Intelligence*, 12:629–639, 1990.

[34] Ramaesh T., Mendis B. R. R. N., Ratnatunga N., and Thattil R. O. Cytomorphometric analysis of squames obtained from normal oral mucosa and lesions of oral leukoplakia and squamous cell carcinoma. *Journal of Oral Pathology and Medicine*, 27(2):83–86, 1998.

[35] Ranefall P. *Towards automatic quantification of Immunohistochemistry using colour image analysis*. PhD thesis, Uppsala University, Uppsala, Sweden., 1998.

[36] Sahoo P.K., Soltani S., and Wong A. K. C. A survey of thresholding techniques. *Computer Vision, Graphics, and Image Processing*, 41(2):233–260, 1988.

[37] Sato Y., Westin C.-F., Bhalerao A., Nakajima S., Shiraga N., Tamura S., and Kikinis R. Tissue classification based on 3d local intensity structure for volume rendering. *IEEE Trans on Visualization and Computer Graphics*, 6(2):160–180, 2000.

[38] Schilling T., Miroslaw L., Glab G., and Smereka M. Towards rapid cervical cancer diagnosis: automated detection and classification of pathologic cells in phase-contrast images. *International Journal of Gynecological Cancer*, 17:118–126, 2007.

[39] Smith S.M. and Brady J.M. Susan - a new approach to low level image processing. *International Journal of Computer Vision*, 23(1):45–78, 1997.

[40] Soille P. *Morphological Image Analysis: Principles and Applications*. Springer-Verlag, pp.170–171, 1999.

[41] Sonka M., Hlavac V., and Boyle R. *Image Processing, analysis, and machine Vision*. Thomson Engineering, 3rd edition, 2007.

[42] Söderberg O., Gullberg M., Jarvius M., Ridderstråle K., Leuchowius K-J., Jarvius J., Wester K., Hydbring P., Bahram F., and Larsson L-G.and Landegren U. Direct observation of individual endogenous protein complexes in situ by proximity ligation. *Nature Methods*, 3:995–1000, 2006.

[43] Stephens D. J. and Allan V. J. Light microscopy techniques for live cell imaging. *Science*, 300:82–86, 2003.

[44] Szczypiński P. M., Strzeleckia M., Materkaa A., and Klepaczkoa A. Mazda-a software package for image texture analysis. *Computer Methods and Programs in Biomedicine*, 2008. Available online, doi:10.1016/j.cmpb.2008.08.005.

[45] Tomasi C. and Manduchi R. Bilateral filtering for gray and color images. 1998. Proceedings of IEEE International Conference on Computer Vision pp. 839–846.

[46] Tsien R. Y. The green fluorescent protein. *Annual Review of Biochemistry*, 67:509, 1998.

[47] Tuceryan M and Jain A.K. *Texture Analysis -Handbook of Pattern Recognition and Computer Vision, C.H. Chen, L.F. Pau and P.S.P.Wang eds.* World Scientific, pp. 235–276, 1993.

[48] Vermolen B.J., Garini Y., Mai S., Mougey V., Chuang T. C-Y. Fest T., Chuang A. Y-C., Wark L., and Young I.T. Characterizing the three-dimensional organization of telomeres. *Cytometry Part A*, 67A:144–150, 2005.

[49] Vermolen B.J., Garini Y., Young I.T., Dirks R.W., and Raz V. Segmentation and analysis of the three-dimensional redistribution of nuclear components in human mesenchymal stem cells. *Cytometry Part A*, 73, 2008.

[50] Vincent L. and Soille P. Watersheds in digital spaces: An efficient algorithm based on immersion simulations. *IEEE Transactions on Pattern Analysis and Machine Intelligence*, 13(6):583–598, 1991.

[51] Vincent L. Morphological grayscale reconstruction in image analysis: Applications and efficient algorithms. *IEEE Transactions on Image Processing*, 2(2):176–201, 1993.

[52] Wählby C. and Bengtsson E. Segmentation of cell nuclei in tissue by combining seeded watersheds with gradient information. *Proceedings of SCIA-03: Scandinavian Conference on Image Analysis, LNCS 2749*, pages 408–414, 2003.

[53] Wählby C., Sintorn I-M., Erlandsson F., Borgefors G., and Bengtsson E. Combining intensity, edge and shape information for 2d and 3d segmentation of cell nuclei in tissue sections. *Journal of Microscopy*, 215:67–76, 2004.

[54] Zhang B., Zerubia J., and Olivo-Marin J. Gaussian approximations of fluorescence microscope point-spread function models. *Applied Optics*, 46:1819–1829, 2007.

[55] Åhlen J. *Colour correction of underwater images using spectral data*. Colour correction of underwater images using spectral data. PhD thesis, Uppsala University, Uppsala, Sweden, 2005.

Acta Universitatis Upsaliensis

Digital Comprehensive Summaries of Uppsala Dissertations from the Faculty of Science and Technology 596

Editor: The Dean of the Faculty of Science and Technology

A doctoral dissertation from the Faculty of Science and Technology, Uppsala University, is usually a summary of a number of papers. A few copies of the complete dissertation are kept at major Swedish research libraries, while the summary alone is distributed internationally through the series Digital Comprehensive Summaries of Uppsala Dissertations from the Faculty of Science and Technology. (Prior to January, 2005, the series was published under the title "Comprehensive Summaries of Uppsala Dissertations from the Faculty of Science and Technology".)

Distribution: publications.uu.se
urn:nbn:se:uu:diva-9541

ACTA
UNIVERSITATIS
UPSALIENSIS
UPPSALA
2009